https://doi.org/10.5194/egusphere-2026-4392
Preprint. Discussion started: 10 August 2026

Merging a model of optimal allocation of carbon and nitrogen with one of photosynthesis and respiration

Chris Huntingford[1], Rebecca J. Oliver[1], Lina M. Mercado[2,1], Stephen A. Sitch[2], Douglas B. Clark[1], Annikki Mäkelä[3], Carolina Mayoral[4], and Richard J. Norby[4,5]

[1]U.K. Centre for Ecology and Hydrology, Benson Lane, Wallingford, Oxfordshire, OX10 8BB, U.K.
[2]Faculty of Environment, Science and Economy, University of Exeter, Exeter, EX4 4RJ, U.K.
[3]Institute for Atmospheric and Earth System Research (INAR) & Faculty of Agriculture and Forestry, P.O. Box 27 (Latokartanonkaari 7), FI-00014 University of Helsinki, Finland
[4]Birmingham Institute for Forest Research, University of Birmingham, U.K
[5]Environmental Sciences Division, Oak Ridge National Laboratory, Oak Ridge, TN, USA

Correspondence to: Chris Huntingford (chg@ceh.ac.uk)

Abstract. Knowledge of the evolution of the terrestrial carbon cycle in a changing climate is important for many reasons, including allowing for an assessment of the extent to which the land can partially offset carbon dioxide (CO_2) emissions due to human burning of fossil fuels. However, understanding some characteristics of the response of terrestrial ecosystems to different environmental forcings remains limited. Future detailed measurement campaigns may advance our understanding of ecological processes, but many measurements that are needed to improve model representation have not yet been collected. Furthermore, a prerequisite of large-scale land surface models is their ability to accurately estimate change in all locations, and so will inevitably include places for which data may never be available. This global requirement is due to the need to develop robust predictions of the overall response of how land carbon stores will evolve in response to climate change, despite incomplete information and related unknowns. Global carbon storage on land still continues to increase, compensating for a substantial fraction of anthropogenic carbon dioxide (CO_2) emissions. Quantifying the magnitude of future CO_2 drawdown is critical to determining emissions pathways compatible with climate targets, including limiting global warming to two degrees above preindustrial levels. Designed to reduce uncertainty in terrestrial carbon storage and its interactions with biogeochemical cycles, optimisation hypotheses propose that ecosystems maximise specific attributes such as carbon uptake. If validated, these hypotheses offer a mathematical framework that can replace unknown mechanistic equations in land system models. Furthermore, optimal calculations that represent plant responses to local environmental conditions can capture geographical variations, substituting for spatially incomplete data, and, in particular, additionally provide expected responses to climate change forcings. Here, we substantially extend an existing description of the optimal carbon allocation between the three stores of wood, foliage, and fine root biomass (Makela et al., 2008). This extension incorporates an established model of the photosynthesis response (Farquhar et al., 1980) and the stomatal response (Medlyn et al., 2011) to near-surface meteorological conditions. The original optimal algorithm (Makela et al., 2008) maximises net primary productivity (that is, photosynthesis minus maintenance respiration) by determining how available nitrogen is allocated, which then influences the simulated size of the three carbon stores. In our extended mathematical framework, we first present how optimal allocation and resultant wood,

https://doi.org/10.5194/egusphere-2026-4392
Preprint. Discussion started: 10 August 2026

foliage and fine root store sizes additionally depend on individual changes to near-surface meteorological and climatological drivers. We then estimate projected changes in allocation for the simultaneous increase in temperature and atmospheric CO_2 concentration, representing the effects of global warming. Finally, we evaluate the performance of the revised model in a temperate mature deciduous oak forest, contrasting with its original development for mature boreal evergreen pines. This forest is located at the BIFoR FACE (Birmingham Institute for Forest Research Free Air Carbon Dioxide Enrichment) facility, where continuous monitoring of the response of temperate forest trees to CO_2 has been carried out since 2018 (Foyer et al., 2025). Such data reveal that our enhanced simulation structure performs well in projecting the allocation of carbon to different stores. A key aim of our analysis is to create a mathematical structure for potential inclusion in the terrestrial carbon cycle components of Land Surface Models (LSMs). These models, in turn, may be used in Earth System Models (ESMs), to aid projections by the latter of the global carbon cycle in response to prescribed scenarios of CO_2 emissions.

1 Introduction

The land surface has a major role in the Earth system, responding to and feeding back on near-surface meteorology. Furthermore, terrestrial ecosystems play a substantial role in the global carbon cycle and are currently a net sink for atmospheric carbon dioxide (CO_2) (e.g. Canadell et al., 2007; Friedlingstein et al., 2025) that offsets approximately 21% of CO_2 emissions due to the societal burning of fossil fuels (Friedlingstein et al., 2026). Any changes in levels of atmospheric CO_2 captured by land ecosystems may have strong implications for the ability to meet key climate targets, as this will alter the level of compatible emissions over the coming decades. Such targets may include keeping global warming below two degrees since preindustrial times. Consequently, reliable models of terrestrial carbon cycling are required. These simulations must have a sufficiently complete representation of processes so that they can project changes to land carbon stores in response to any new climate regimes and the related higher atmospheric CO_2 concentrations. Such models also need to be applicable to a range of different background environmental conditions that occur throughout the world so that subsequent spatial averaging can predict the contemporary global mean carbon stores of land and their expected changes in the decades ahead.

Terrestrial carbon cycling depends mainly on how the gains from photosynthesis are distributed between the roots and other components of vegetation (e.g. Franklin et al., 2020; Litton et al., 2007) and while also accounting for losses through respiration. In addition to physical climate drivers that impact terrestrial carbon cycle processes through photosynthesis and respiration, the functioning of the land surface is also strongly dependent on carbon cycle interactions with other geochemical cycles and, most notably, nitrogen (e.g. Zaehle, 2013; Huntingford et al., 2022). Unfortunately, there is currently no complete understanding of how available carbon is allocated among ecosystem components. Medlyn et al. (2015), for example, develop a roadmap for reducing uncertainty in vegetation models, which may ultimately occur by using comprehensive sets of FACE experiment measurements, citing the dynamic allocation of carbon as a key unknown. However, in the current absence of available data, and to address this incomplete information, including the related lack of a full set of descriptive equations, one possibility is to use simultaneous measurements to build empirical descriptions of ecological processes. These descriptions can include interaction between components and, in particular, with environmental drivers. However, while such a procedure

https://doi.org/10.5194/egusphere-2026-4392
Preprint. Discussion started: 10 August 2026

can provide valuable insights based on contemporary data, empirical relations may lack robust predictive capability for out-of-sample forcings such as imposed climate change. An alternative intermediate approach exists, falling between empirical fitting and full knowledge of ecosystem effects, where the latter is currently unavailable due to the lack of a completely closed set of equations. This middle method employs the concept that some vegetation behaviours likely follow optimal pathways by maximising a particular physiological attribute. Optimisation brings three advantages. First, it generates effective (implicit) descriptions of processes where knowledge is lacking. A mathematical interpretation is that optimisation may complete (i.e. close) the set of equations in a land model, compensating for missing equations due to gaps in process understanding. Such a closure is appealing for describing plant carbon allocation, where the mechanisms are not yet fully resolved. Second, under the assumption that optimal behaviour remains valid under altered conditions or forcings, this enables predictions for changed climatic conditions. Third, under the additional assumption that any optimisation hypothesis holds for geographically varying locations, this enables calculations for the many places where data are unavailable for land model calibration. The latter feature is useful when developing land surface models such as Dynamic Global Vegetation Models (DGVMs) (e.g. Sitch et al., 2008, 2024), designed to be globally applicable.

Ultimately, DGVMs are required as a land component in Earth System Models (ESMs), which are used to simulate the full climate-carbon cycle system response to fossil fuel burning, supporting statements in the reports of the Intergovernmental Panel on Climate Change (e.g. IPCC, 2013, 2021). All ESMs require a surface scheme that describes land-atmosphere exchanges of momentum, heat, vapour and CO_2. However, many ESMs extend previous climate models by allowing forcing with scenarios of future CO_2 emissions rather than atmospheric CO_2 concentrations. As such, ESMs link emission rates directly to climate change, which is often more useful to policymakers. For ESMs to perform emissions-driven calculations, they require a fully interactive representation of the global carbon cycle, including the simulation of evolving land carbon stores by DGVMs. Some ESMs that simulate the carbon cycle have been available for more than two decades (e.g. Cox et al., 2000), but uncertainty remains about how land carbon stores will alter under climate change.

To support DGVM development, many land-based optimisation hypotheses are available (e.g. Harrison et al., 2021) and some authors offer mathematical models that translate these conjectures into equation form. Here, we adopt the optimisation model of Makela et al. (2008), which dynamically determines the ratio of carbon allocation among fine roots, foliage and wood. This model operates on the assumption that trees optimise their use of available resources, which, in this context, involves the allocation of available carbon to these three components in order to achieve the highest productivity by maximising Net Primary Productivity (NPP), i.e. photosynthesis minus respiration. Specifically, to achieve optimality, there is an intermediate control variable, foliage nitrogen, for which a specific value will maximise NPP. The carbon gains from increased nitrogen availability (which enables enhanced photosynthesis) are balanced against the carbon costs of increased nitrogen uptake (i.e. higher maintenance respiration and fine root construction). This balance also depends on an overall prescribed maximum rate of nitrogen uptake by the roots, which acts as an external forcing boundary condition.

The optimal NPP model used by Makela et al. (2008) has, however, limited environmental dependencies. In particular, the model does not include the influence of near-surface climatology or the direct impact of atmospheric CO_2 concentration on NPP. Here, we merge the optimal model with a slightly modified version of the well-established "Farquhar" description of pho-

https://doi.org/10.5194/egusphere-2026-4392
Preprint. Discussion started: 10 August 2026

tosynthesis (Farquhar et al., 1980). The model proposed by (Farquhar et al., 1980) itself requires an additional closure equation to provide a value for leaf internal CO_2 concentration, c_i. This extra equation pertains to stomatal conductance, and here we select the conductance model of Medlyn et al. (2011), itself an optimality-based approach. Combined, this new framework introduces additional dependencies of leaf-level temperature, light availability, vapour pressure deficit, and atmospheric CO_2 concentration into the Makela et al. (2008) optimal concept framework. Furthermore, we introduce an overall dependence of NPP on soil moisture similar to that presented in Eq. (11) of Best et al. (2011). Lastly, we provide a more complete description of plant respiration, based extensively on the model given in Clark et al. (2011), which includes a dependence on leaf-level temperature and soil moisture.

Our novel approach to simulation combines an optimisation method for carbon allocation with descriptions of photosynthesis and respiration. We examine its responses to meteorological drivers representative of a Finnish pine forest site. We adopt the existing physiological parameters to align with the original Makela et al. (2008). We explore how the model responds to individual variations in environmental drivers, and then consider the simultaneous variation of temperature and CO_2 concentration representative of future climate conditions. Lastly, we apply the revised model to a different ecosystem, that of a mature broadleaf deciduous temperate forest. We use data from the Birmingham Institute for Forest Research (BIFoR) Free-Air CO_2 Enrichment (FACE) experiment (Hart et al., 2020), at such a forest, to parameterise and evaluate the model under ambient and future CO_2 conditions. This final step is an initial stage towards the approach suggested by (Medlyn et al., 2015). Importantly, this last step can benefit from the longer timescales associated with FACE experiments and that are also associated with allocation effects.

2 Methods and Data

2.1 Summary of the model of optimisation and its combination with a full photosynthesis model and adjusted plant respiration model

Our aim is to extend the optimal carbon allocation model of Makela et al. (2008) to account for dependencies on local climatological conditions. These conditions are introduced by incorporating a more realistic description of photosynthesis and respiration into the optimal model, along with a description of stomatal opening. These amendments lead to a dependence on surface temperature, humidity, and light levels, as well as a response to atmospheric CO_2 levels and soil moisture status. We now present the revised equation set.

2.1.1 The optimisation model and its extension

The overarching calculation of the optimal allocation model of Makela et al. (2008) is to determine a dimensionless value ϕ_r, which is the ratio of fine root biomass, W_r (kg DM ha^{-1}), to foliage biomass, W_f (kg DM ha^{-1}) (i.e. $\phi_r = W_r/W_f$), where "DM" stands for dry matter. The optimal calculation also determines wood biomass, W_w (kg DM ha^{-1}), where we note in this model that wood biomass refers to sapwood. The complete set of equations leading to the calculation of the values of

https://doi.org/10.5194/egusphere-2026-4392
Preprint. Discussion started: 10 August 2026

ϕ_r is presented predominantly in Makela et al. (2008), and particularly in the Supplemental material of that analysis. A brief summary of the ϕ_r calculation is as follows. The first requirement is to prescribe a key model forcing, via the parameter σ_{rM} (kg N (t fine root)$^{-1}$ yr^{-1}), which is the maximum fine root-specific rate of N uptake (the 'x'-axes of the panels of Fig. S3 in Makela et al. (2008)). With knowledge of this value, the allocation model is fully defined, except that the number of process equations is one less than the number of variables that require solution. In mathematical terminology, the model contains "an unconstrained extra degree of freedom". However, if a value of foliage nitrogen, $[N]_f$ (kg N (kg DM foliage)$^{-1}$) is known, then all equations are solvable, including generating a value for ϕ_r. Knowledge of $[N]_f$ also predicts G (kg DM ha^{-1} yr^{-1}), which is the rate of production of new DM. Quantity $G = Y(P - R_m)$ is a rate of production and where P (kg C ha^{-1} yr^{-1}) is the rate of photosynthesis, R_m (kg C ha^{-1} yr^{-1}) is the rate of maintenance respiration and Y (kg DM (kg C)$^{-1}$) converts from carbon to dry matter accounting for losses to growth respiration. Hence, with $G = G(\phi_r([N]_f), [N]_f)$, the optimal hypothesis of Makela et al. (2008) is that vegetation adjusts its $[N]_f$ value to maximise G, and in doing so, determines ϕ_r. The assumption of maximising G provides the extra degree of freedom missing and thus determines the unique values of $[N]_f$ and thus ϕ_r. The solution to the optimisation calculation enables the calculation of λ_f, λ_r and λ_w, which are the allocation fractions of G to each of the three components.

Our aim is to retain, as far as possible, the main features of the optimal model, as expressed through the equations in Makela et al. (2008). In particular, our approach is to introduce dependencies on local climatological conditions through revised models of P and R_m while preserving the original dependencies of the model components on the foliage nitrogen concentration levels. Keeping these nitrogen dependencies, we continue to solve the cubic algebraic equation for ϕ_r (i.e. Eqn S10; Makela et al., 2008), where the coefficients of that cubic depend on $[N]_f$. The optimisation method remains that of selecting a $[N]_f$ value such that the related (highest real value) solution to the cubic equation corresponds to the largest possible value of production, G. To allow local climatological conditions to drive our revised model, we calculate the annual mean daytime meteorological conditions over the period from 1996 to 2014, inclusive, at the Hyytiala forest eddy covariance flux tower site in Finland, which is dominated by needleleaf evergreen trees (Fi-Hyy; https://fluxnet.org/sites/siteinfo/FI-Hyy). These calculations give annual mean conditions of air temperature = 5.74 ^{o}C, shortwave radiation = 134.6 Wm^{-2}, specific humidity = 0.0049 kg kg^{-1}, CO_2 concentration = 397 ppm and we assume no soil moisture stress. We initially select a Finnish site as this aligns well with the original paper of (Makela et al., 2008). Following this, we also perform calculations relevant to the BIFoR-FACE location in the United Kingdom.

2.1.2 Enhanced model of photosynthesis

We introduce a more sophisticated description of photosynthesis, P, as follows. The existing format is that $P = P(W_f, [N]_f)$. The first dependency on W_f (kg DM foliage ha^{-1}) is provided by Makela et al. (2008); their Eqn (6):

$$P = \frac{\sigma_{fM} W_f K_f}{W_f + K_f} \tag{1}$$

https://doi.org/10.5194/egusphere-2026-4392
Preprint. Discussion started: 10 August 2026

where σ_{fM} (kg C (kg DM foliage)$^{-1}$ yr^{-1}) is defined as a "light-saturated foliage-specific rate of photosynthesis". For the second dependency, the quantity σ_{fM} depends on $[N]_f$ as:

$$\sigma_{fM} = \frac{\sigma_{fM0}[\mathrm{N}]_\mathrm{p}}{[\mathrm{N}]_\mathrm{p} + [\mathrm{N}]_\mathrm{ref}}, \qquad [\mathrm{N}]_\mathrm{p} = \max\{[\mathrm{N}]_\mathrm{f} - [\mathrm{N}]_0, 0\}, \tag{2}$$

and where K_f (kg DM foliage ha^{-1}) , σ_{fM0} (kg C (kg DM foliage)$^{-1}$ yr^{-1}), $[N]_{ref}$ (kg N (kg DM foliage)$^{-1}$) and $[N]_0$ (kg N (kg DM foliage)$^{-1}$) are parameters. See Makela et al. (2008); their Eqn (10).

We first propose that Eq. (1) broadly captures leaf-to-canopy scaling. This scaling is more frequently presented as a function of the Leaf Area Index (LAI) (m^2 m^{-2}), and represents a form of integration within the canopy of decaying photosynthetic strength for deeper vegetation layers (e.g. Sellers et al., 1992). These mappings begin to saturate, therefore, at higher LAI values. Here, instead, such saturation is modelled in W_f (rather than LAI). We retain Eq.(1), and therefore interpret σ_{fM} as a quantity describing the top leaf-level photosynthesis.

Second, in our adjustments to introduce a photosynthesis model, our objective is to retain as much of the nitrogen influence as given by Eq. (2), thus preserving links to the methodology of Makela et al. (2008). We introduce new environmental dependencies of photosynthesis within σ_{fM0}, thereby transforming the way this quantity is modelled from being a fixed parameter to a variable. However, many descriptions of photosynthesis also contain a nitrogen dependency. Hence, our aim is to keep that particular process description and dependency external to the variable σ_{fM0}, ideally following or resembling Eq. (2) and thus again consistent with Makela et al. (2008).

Specifically, we replace σ_{fM} with a photosynthesis model $A^* = \min(A_v, A_j)$ (kg C kg leaf^{-1} yr^{-1}) and that has no nitrogen limitation. A_v is Rubisco-limited photosynthesis, while A_j is light-limited photosynthesis, and both variables follow the model of Farquhar et al. (1980). The exact suggested equation format is given by Eqs. (2), and (3) with (4) of (Oliver et al., 2022) for A_v and A_j respectively. This introduces a dependence on temperature (^{o}C) for both photosynthetic components, and for A_j there is a dependence on light Q (W m^{-2}). Both photosynthetic rates depend on c_i, which is the intercellular concentration of CO_2 (ppm). We link c_i to atmospheric CO_2 concentration implementing the Medlyn model of stomatal conductance, (Medlyn et al., 2011), by using the form of Eq. (9) of Oliver et al. (2022). The model of stomatal conductance additionally introduces a dependence on vapour pressure deficit, d_q (kg kg^{-1}). The descriptions of A_v and A_j depend on V_{cmax} and J_{max} respectively, which is how the temperature dependence is included (see Eq. 5 of Oliver et al., 2022). We additionally scale photosynthesis by a parameter β, which is in the range between zero and one, and represents soil moisture stress. Conditions of no stress correspond to $\beta = 1$.

Although the photosynthetic model presented in Oliver et al. (2022) does not contain an explicit dependence on nitrogen levels in the vegetation components, there is a dependence on leaf nitrogen concentration within the calculation of V_{cmax}. Furthermore, J_{max} is routinely modelled as linear in V_{cmax}, and so this nitrogen dependence will also appear in this variable. In Harper et al. (2016), a linear dependence on this foliar nitrogen is assumed, although the gradient of the response is dependent on Plant Functional Type (PFT). Other authors suggest instead a saturation of photosynthesis in increasing nitrogen concentration (for instance, the references cited in Makela et al. (2008) of Field and Mooney (1986), Hilbert (1990), Franklin and Ågren (2002) and Ellsworth et al. (2004)), which gives a mathematical form that closely resembles or exactly matches that of Eq. (2).

https://doi.org/10.5194/egusphere-2026-4392
Preprint. Discussion started: 10 August 2026

Hence, within our equation for V_{cmax}, we set this as the prescribed parameter value used in the JULES model (Harper et al., 2016). The value is prescribed as 0.01083 (kg N kg leaf^{-1})) for leaf nitrogen concentration and for the needleleaf tree PFT, which is a high value and so assumes no nitrogen limitation within the A^* model. This approach then allows us to introduce an external modification of A^* for nitrogen availability, although using the saturating form, i.e. Eqn (2). That is, σ_{fM} tends to a constant for large and increasing values of $[N]_p$, rather than a linear dependency. (This introduction of nitrogen directly on the photosynthesis model, rather than indirectly via V_{cmax}, has one additional implication. For Rubisco-limited photosynthesis, A_v is linear in V_{cmax}, whereas light-limited photosynthesis, A_j, is not strictly linear in J_{max} i.e. the potential rate of electron transport, for particularly low light levels (e.g. solving Eqs. 3 and 4 of Oliver et al., 2022).

Combining all these considerations gives an assumed multiplicative relationship between both A_v and A_j and a saturating dependence on nitrogen concentration (Eq. (2)), the use of Eq. (1) to characterise canopy scaling, as well as a scaling for soil moisture. Critically, this approach also introduces near-surface climate conditions through the photosynthesis model represented by A^*. Together, this gives:

$$P = \underbrace{\beta \times A^*(T, Q, d_q, c_a)}_{\text{New effective parameter } \sigma_{fM0}} \times \underbrace{\frac{[\mathrm{N}]_\mathrm{p}}{[\mathrm{N}]_\mathrm{p} + [\mathrm{N}]_\mathrm{ref}} \times \frac{W_f K_f}{W_f + K_f}}_{\text{From original model}}, \qquad [\mathrm{N}]_\mathrm{p} = \max\{[\mathrm{N}]_\mathrm{f} - [\mathrm{N}]_0, 0\}. \tag{3}$$

Eq (3) introduces a temperature, light, vapour pressure deficit, CO_2 concentration and soil moisture stress dependency into the modelled photosynthesis, P, of the optimal model. In Fig. S3 of Makela et al. (2008), a sensitivity to CO_2 is presented, depending on the perturbation of the parameters σ_{fM0} and the allometric quantity c_H. Here, our new dependencies offer a more process-led basis for determining variations in σ_{fM0} corresponding to different CO_2 levels (although the c_H dependence may be more closely related to changed long-term allometric behaviours at higher carbon dioxide levels, which our revised model does not capture). The parameter values required by the photosynthesis model are sourced from (Oliver et al., 2022) and for the needleleaf evergreen tree PFT. The photosynthesis model, driven by the local climatological conditions of the Fi-Hyy flux site, predicts that P is 9.8 kg C kg leaf^{-1} yr^{-1}, which is the same order-of-magnitude as σ_{fM0} when estimated by the original Makela model of 4 kg C kg leaf^{-1} yr^{-1} at the same leaf N concentration.

2.1.3 Model of plant respiration

Similarly to photosynthesis, our aim is to map a new functionality to the model of Makela et al. (2008) so that it introduces a dependence on temperature and soil moisture in the description of respiration, both of which are known to affect this component of terrestrial carbon cycling. By mirroring our approach to photosynthesis, we wish to add these new environmental dependencies while retaining the mathematical structure of the optimal solution, as presented in the Supplementary material of (Makela et al., 2008). Specifically, we plan to maintain all the algebra that leads to solving a cubic equation for the ratio ϕ_r, subject to nitrogen allocation $[N_f]$ that maximises $G = Y(P - R_m)$. Thus, for respiration, we need to retain a similar dependence on $[\mathrm{N}]_\mathrm{f}$, $[\mathrm{N}]_\mathrm{r}$ and $[\mathrm{N}]_\mathrm{w}$ as in the original model, which takes the form of

$$R_m = r_m \left([\mathrm{N}]_\mathrm{f} \mathrm{W}_\mathrm{f} + [\mathrm{N}]_\mathrm{r} \mathrm{W}_\mathrm{r} + [\mathrm{N}]_\mathrm{w} \mathrm{W}_\mathrm{w} \right). \tag{4}$$

https://doi.org/10.5194/egusphere-2026-4392
Preprint. Discussion started: 10 August 2026

Here r_m (kg C (kg N)$^{-1}$ yr^{-1}) is a parameter, and subscripts f, r, w denote foliage, fine roots and live wood. We therefore consider the feasibility of retaining this direct N-dependence, while modulating the parameter r_m to include a dependence on near-surface meteorology, and specifically on temperature T and soil moisture θ.

To derive a more complete response for R_m, we first consider the respiration equations used in the JULES model (which is an LSM with many uses, including application in ESMs; Clark et al. (2011)). At the top leaf level, the JULES model describes maintenance respiration (named R_{pm} in that model) as:

$$R_{pm} \propto R_d \left(\beta + \frac{N_r^J + N_s^J}{N_l^J} \right). \tag{5}$$

Here β is again a factor between zero and unity used to quantify soil moisture stress (with unity being no stress), and N_r^J, N_s^J and N_l^J are the nitrogen concentrations in the JULES model for fine roots, stems, and leaves, respectively. The parameter R_d is linear in $V_{cmax,25}$, i.e.

$$R_d \propto V_{cmax,25}.$$

R_d is also linear in a function of temperature, which follows the form given in Eq. (5) of Oliver et al. (2022) and is repeated here:

$$R_d \propto e^{H_a(T-T_{\rm ref})/(T_{\rm ref}RT)} \times \frac{\left(1+e^{(T_{\rm ref}\Delta S - H_d)/(T_{\rm ref}R)}\right)}{\left(1+e^{(T\Delta S - H_d)/(TR)}\right)}. \tag{6}$$

Here, $T_{\rm ref} = 298.15$K (i.e. 25°C), while $H_a, R, \Delta S$ and H_d are parameters described in Oliver et al. (2022).

Importantly, $V_{cmax,25}$ is itself dependent on nitrogen level. As noted in Section 2.1.2, one dependence of this parameter on nitrogen (e.g. Eq. (6) of Clark et al. (2011) and Eq. (3) of Harper et al. (2016)) is where the JULES model sets $V_{cmax,25}$ as linear in leaf nitrogen, N_l^J, i.e.:

$$V_{cmax,25} \propto N_l^J. \tag{7}$$

A linearity in nitrogen concentration aligns with Eqn (4), and therefore as used in the original model of Makela et al. (2008). Hence, our approach is similar to that for photosynthesis, which is to assume that nitrogen availability takes a relatively high fixed value in the calculation of $V_{cmax,25}$, while retaining the actual nitrogen dependence as an extra response, external to that parameter. This response is taken to be similar to that of Eqn (4), although such linearity for respiration implies a different dependence of $V_{cmax,25}$ on nitrogen compared to the saturating form used for photosynthesis in Eq. (3). We suggest that although it is often common for models of photosynthesis and respiration to use the same "V_{cmax}" forms for both, there is no overall process or data-led reason for such a commonality.

We make three further assumptions of: (i) in Eq. (5), $N_r^J \sim N_s^J \sim N_l^J$, (which creates a factor of two, and removes the nitrogen dependency present in Eq. (5)); (ii) an overall scaling of respiration in soil moisture represented by parameter β, and (iii) the leaf-to-canopy scaling is captured by the linearity in the biomass components (i.e. W_f, W_r and W_w) of Eq. (4). This linearity for respiration contrasts with the exponential decay within a canopy for photosynthesis described in Eq. (1).

https://doi.org/10.5194/egusphere-2026-4392
Preprint. Discussion started: 10 August 2026

Combining all the factors above results in a new respiration description that expands the Makela model as:

$$R_m = \underbrace{\mu_R \beta(\beta+2) \times e^{H_a(T-T_{\mathrm{ref}})/(T_{\mathrm{ref}}RT)} \times \frac{\left(1+e^{(T_{\mathrm{ref}}\Delta S - H_d)/(T_{\mathrm{ref}}R)}\right)}{\left(1+e^{(T\Delta S - H_d)/(TR)}\right)}}_{\text{Scalar correction to original parameter } r_m} \times \underbrace{r_m \left(\mathrm{N_f W_f} + \mathrm{N_r W_r} + \mathrm{N_w W_w}\right)}_{\text{From original model}} \quad (8)$$

and where μ_R is a multiplicative parameter.

We derive the value of the unitless parameter μ_R such that it returns the same value for canopy-level respiration, R_m, as that for the parameters set in Makela et al. (2008). To obtain equivalence, we assume for their typical Finnish location that $\beta = 1$ (i.e., no soil moisture deficit) and an annual mean daytime temperature of 278.89 (K) derived from the temperature at the Finnish flux tower site Fi-Hyy as described earlier. This fitting yields $\mu_R = 6.0$.

2.1.4 Summary of new mathematical dependencies of the revised optimal model

As outlined above, we have retained the main features of the original optimal model of Makela et al. (2008), as described in their Supplementary Material. We have changed the parameter σ_{fM} to instead be a function of climate-related dependencies via a description of photosynthesis based on the established "Farquhar" model. This modification we name as $\sigma^*_{fM0} = \beta \times A^*(T, Q, d_q, c_a)$, marked as "new effective parameter" in Eqn (3). We have also introduced environmental dependencies into the respiration model by adjusting the parameter r_m, marked as "scalar correction to original parameter r_m" in Eqn (8). Writing the product of the scalar and r_m as r^*_m, from Eqn (8) yields $R_m = r^*_m \left(\mathrm{N_f W_f} + \mathrm{N_r W_r} + \mathrm{N_w W_w}\right)$. Our new dependencies can be summarised as:

$$\sigma^*_{fM0} = \sigma^*_{fM0}(T, I, D, c_a, \beta(\theta)), \quad (9)$$

$$r^*_m = r^*_m(T, \beta(\theta)), \quad (10)$$

where θ ($\mathrm{m^3}$ water ($\mathrm{m^3}$ soil)$^{-1}$) is soil moisture. Although Eq. (9) introduces five external environmental drivers, Eqs. (9) and (10) act as just two immediate variables, necessitating the calculation of σ_{fM} and r^*_m at each location. We also note that, as in the original model form, each location requires a value of overall N-uptake (i.e. the value of σ_{rM}). Hence, mathematically, our revised model possesses three degrees-of-freedom, and if each of these three quantities is set, a unique value for parameter ϕ_r is calculated, that is:

$$\phi_r = \phi_r(\sigma_{rm}, \sigma_{fM}, r^*_m). \quad (11)$$

In reality, there are many more degrees-of-freedom because all model parameters, both in the original model components and in the introduced photosynthetic and respiration responses, may be biome-specific (e.g. see the description of BIFoR data below, Section 2.2).

It is noted that we assume a response to annual mean values of environmental forcings in the calculations. First, the model of Makela et al. (2008), and our extension here, are equilibrium calculations, i.e., the model contains no time derivatives. If we instead forced the model with time-evolving mean meteorological quantities calculated at the seasonal timescale or shorter, this would lead to unrealistic major variations in allocation and thus carbon stores. We consider this issue of a lack of inertial

https://doi.org/10.5194/egusphere-2026-4392
Preprint. Discussion started: 10 August 2026

equation terms in the model, alongside other caveats, in more detail in Section 4. Furthermore, the mean temperature adopted from the Finnish site is from the height of the meteorological measurements, rather than that at leaf level.

2.2 BIFoR data

Moving from the mature evergreen pine stands of Finland, we next apply our revised optimal model to describe the mature broadleaf deciduous temperate forest stand at the Birmingham Institute of Forest Research (BIFoR) site in the UK (MacKenzie et al., 2021). This site is dominated by 175-year old English oak trees (*Quercus robur*) and, critically, includes a Free Air CO_2 Enrichment facility (FACE). Therefore, substantial data are available on the growth of these mature trees under both ambient and elevated CO_2 conditions (Norby et al., 2024b). Hence, this site allows us to test our revised model in a biome different from that of the Finnish site, and, importantly, to evaluate the performance of the model for elevated CO_2 concentrations. Different background CO_2 concentrations are a new forcing we introduce (c_a in Eqns (3) and (9)).

We re-parameterised the model for the BIFoR-FACE location using site observations where possible, for trees grown at ambient CO_2 levels. Values are presented in Table 1. The values of the parameters T_f, T_r, r_m, n_r, f_f, f_r, and f_w are taken directly from observations at the BIFoR-FACE site. The mean lifetime of the foliage, T_f, is set at 1.0 because these deciduous oak trees have one set of leaves per year. The quantity T_r, the mean lifetime of fine roots, are calculated from measurements of fine-root production and biomass, as described in (Norby et al., 2024b). The variable r_m, the specific rate of respiration, is calculated from the mean dark respiration rate (μmol m^{-2} s^{-1}) as measured in year 2022 and converted to the correct units using measured Leaf Mass per unit Area (LMA) (kg m^{-2}) and the nitrogen content of the leaves (kg N kg $leaf^{-1}$) (C. Mayoral, unpublished data). The quantities f_f, f_r and f_w, the proportion of N recycled, are calculated for leaves and assumed to be the same for fine roots and wood (C. Mayoral, unpublished data). The parameter n_r, the ratio of fine root to leaf nitrogen, is derived directly from the average nitrogen (percent) measured in green leaves and fine roots, collected over the period 2016 to 2022 (leaves) and 2018 to 2022 (fine roots, down to a depth of 30cm), (C. Mayoral, unpublished data). The concentration of photosynthetic N, N_{ref}, is calculated under the assumption that 18 % of total leaf N is photosynthetic N, according to Luo et al. (2021). When observations were not available, we make reasoned estimates. For example, the allometric parameters C_h and a_w are important for determining biomass, and we would expect these to be different for evergreen compared to deciduous habits. The quantity C_h is essentially a height parameter, so we reduce this compared to the value for pines, as oaks tend to be shorter. However, we increase the value of the parameter a_w on the basis that oaks are ring-porous hardwood species with a denser sapwood compared to needleleaf evergreen trees. Our simulation framework is based on a description of photosynthesis that replaces the requirement to specify the parameter σ_{fM0}. Instead, therefore, we use measured values of $V_{cmax,25}$, $J_{max,25}$ (Gardner et al., 2022) and LMA from the oak trees at BIFoR (R. J. Norby, unpublished data), as required by the newly implemented Farquhar et al. (1980) photosynthesis scheme. The revised parameters for all other variables applicable to BIFoR are also presented in Table 1.

Although the optimisation concept assumes that vegetation acts to adjust nitrogen allocations to maximise productivity, there remains a requirement to specify the overall nitrogen availability, σ_{rm} (Eqn (11)). For the BIFoR site, we estimate σ_{rm} from the nitrogen requirements of the trees for growth. We use the approaches of Finzi et al. (2007) and Zaehle (2013), along with

https://doi.org/10.5194/egusphere-2026-4392
Preprint. Discussion started: 10 August 2026

Eqn (9) in the original analysis of Makela et al. (2008), to provide a range of estimated values for σ_{rm}. The methods of Finzi et al. (2007) and Zaehle (2013) calculate nitrogen uptake from observations of nitrogen content and production minus the amount of nitrogen resorbed from the canopy. This "top down" method is necessary as σ_{rm} is essentially an aggregate parameter designed to capture the overall availability of nitrogen to plants as the outcome of multiple different processes. This quantity includes the rate of turnover of the nitrogen pool in the soil and the ease with which the roots absorb nitrogen, which in turn depends on mycorrhizal activity in the soil and associations with the roots. Therefore, σ_{rm} does not have a direct link to measurements and is instead inferred as above. This approach leads to an estimated range of nitrogen availability for BIFoR of between 39 and 69 kg N (t fine root)$^{-1}$ yr^{-1}.

We drive the optimal model using the annual average meteorological conditions for the BIFoR site, albeit here using only mean daytime values. These averages are calculated over the period of years 2002 to 2018, returning values of annual mean air temperature at 11.98 (^{o}C), shortwave radiation at 209.20 (W m^{-2}), specific humidity at 0.0067 (kg kg^{-1}), ambient CO_2 concentration at 397 (ppm) and we assume no soil moisture stress. For the part of the BIFoR experiment with elevated CO_2 concentration, this is set at $c_a = 550$ ppm. We evaluate the behaviour of our revised model against the total measured NPP (dry weight, G), calculated as the mean of measurements taken in years 2021 and 2022 (Norby et al., 2024b). Notably, we conduct this comparison for both ambient and elevated CO_2 FACE rings. NPP measurements during the same period are available for the different pools to calculate the fraction of carbon allocated to foliage (NPP measurements for leaves and reproduction combined), wood (NPP measurements for stem and coarse roots combined) and fine roots (Norby et al., 2024b). The biomass (dry weight) of each pool (leaf, W_f; wood, W_w; and fine root, W_r) is also used in the evaluation and is calculated as described in (Norby et al., 2024b) for both ambient and elevated CO_2 FACE rings. For wood biomass (Norby et al., 2024a), we report the mean across all rings as this represents the accumulated growth over the 180 year lifespan of the oak trees. Leaf nitrogen content is measured as the average nitrogen (%) in green leaves collected from 2016 to 2022, which we use to evaluate $[N]_f$ (C. Mayoral, unpublished data).

3 Numerical Results

We first consider model projections using annual mean meteorological conditions from the Finnish flux tower site ("Fi-Hyy") (Section 2.1.1). These conditions serve as our baseline, as they match the simulated location of the original Makela et al. (2008) analysis that is based on Finnish Pine and Spruce vegetation. For the model components used that originate from the original study, we apply identical parameterisations. We investigate the impact of perturbing individual environmental conditions away from that climatological baseline. We also perturb temperature and CO_2 concentration simultaneously, potentially representing global warming effects. We then change location and examine the performance of the model at the BIFoR UK site (MacKenzie et al., 2021). As described in Section 2.2, this second site includes CO_2 enrichment experiments against which we can test model projections for higher carbon dioxide levels and with our new combined simulation structure.

https://doi.org/10.5194/egusphere-2026-4392
Preprint. Discussion started: 10 August 2026

Parameter	Definition	BIFoR Value	Units	Source
K_r	Amount of fine roots capturing 50% of available N	4500	kg ha^{-1}	-
K_f	Amount of foliage capturing 50% of maximum C gain	4000	kg ha^{-1}	-
T_f	Mean lifetime of foliage	1.0	yr	Observed
T_r	Mean lifetime of fine roots	1.18	yr	(Norby et al., 2024b)
T_s	Mean lifetime of sapwood	45.0	yr	-
Y	Growth efficiency	1.54	kg DW (kg C)$^{-1}$	-
r_m	Specific rate of maintenance respiration	101.75	kg C (kg N)$^{-1}$ yr^{-1}	(C. Mayoral, unpub. data)
n_r	Ratio of fine root N to foliage N	0.4	( )	(C. Mayoral, unpub. data)
n_w	Ratio of sapwood N to foliage N	0.06	( )	-
f_f, f_r, f_w	Proportion of N recycled	0.386	( )	(C. Mayoral, unpub. data)
a_w	Sapwood weight per unit foliage and pipe length	2.75	m^{-1}	-
c_H	Steady-state pipe length coefficient	1600	m (kg N)$^{-1}$ (kg foliage)$^{-1}$	-
N_0	Concentration of non-photosynthetic N	0.02	kg N (kg foliage)$^{-1}$	-
N_{ref}	Concentration of photosynthetic N	0.005	kg N (kg foliage)$^{-1}$	(C. Mayoral, unpub. data)
$V_{cmax,25}$	Maximum carboxylation capacity	61.64	μmol CO_2 m^{-2} s^{-1}	(Gardner et al., 2022)
$J_{max,25}$	Maximum rate of electron transport	115.38	μmol CO_2 m^{-2} s^{-1}	(Gardner et al., 2022)
LMA	Leaf mass per unit area	0.0668	kg m^{-2}	(R. Norby, unpub. data)

Table 1. Parameter values for BIFoR location. The last column indicates whether the parameter value is directly from measurements, or is a best estimate (marked with a dash). DW is Dry Weight.

3.1 Response of the revised optimal model to changes in single environmental forcings at a Finnish location

Our initial results are calculations of the model response to single perturbations in the prescribed annual mean environmental forcings. The impact on the optimal allocation model from varying meteorological conditions is now possible since we have integrated a model of photosynthesis and respiration (Section 2.1.2 and 2.1.3 respectively; see also Eqns. (3) and (8)) that amend the optimal framework of Makela et al. (2008). As noted in those two sections, our new combined model is parameterised such that when driven by the Finnish mean climatology from the Fi-Hyy flux tower site, the projections of carbon allocation are numerically similar to those of the original model (which was also calibrated for Finland; Makela et al. (2008)). To explore the response of the revised optimal model to changes in individual environmental forcings, we set these climatological driver values as our default baseline. We also fix the "midpoint" value of available nitrogen as $\sigma_{rM} = 30$ kg N (t fine root)$^{-1}$ yr^{-1}. The other parameters specific to the components of the optimal model of Makela et al. (2008) are retained as the values given in that reference. Our first perturbation is in the available nitrogen, σ_{rM}, to allow a direct comparison with similar calculations in Makela et al. (2008). We then scan across individual changes in the environmental forcings of temperature, downward shortwave radiation, specific humidity, soil moisture stress and atmospheric CO_2 concentration to illustrate their effect on

https://doi.org/10.5194/egusphere-2026-4392
Preprint. Discussion started: 10 August 2026

optimal carbon allocation predictions (Fig. 1). We present projections, derived from these factorial calculations, of changes in the three vegetation components of wood, foliage and fine roots. The left-hand column of Fig. 1 displays the values of production allocations, λ_f, λ_r and λ_w, for each component (expressed as a percentage) and as a function of the perturbed value of σ_{rM} or environmental condition. The right-hand column is the corresponding biomass changes of each component (t ha^{-1}).

The optimisation calculations predict that as overall nitrogen, N, availability increases, the fractional allocation of carbon, C, to fine roots decreases (Fig. 1a). This calculation agrees with observations that as the N supply becomes more freely available, plants do not need to invest as much, as a fraction of G, in their fine root system to extract what they need to supply nitrogen to the canopy. Instead, the available C can be allocated to the wood pool and to the leaves. For increasing nitrogen availability, wood and foliage biomass are predicted to increase monotonically (Fig. 1b).

Starting with physiological responses to near-surface meteorological conditions, the allocation remains relatively constant for increasing temperatures until about 15 ^{o}C, after which strong nonlinear changes occur (Fig. 1c). The biomass pools are projected to start declining at this temperature point (Fig. 1d). For pine trees found in cool climates, the optimal temperature for photosynthesis is low, and although background temperatures are increasing, the (fixed) light level remains low. Hence, above 15 ^{o}C photosynthesis begins to decrease while respiration remains high, causing the trees to start losing carbon. Therefore, the optimisation calculations invest carbon in foliage and wood to promote growth (for example, by increasing the ability to capture light, which is a limiting resource). There is only a small sensitivity to the perturbation of downward shortwave radiation. A small increase (decrease) is observed in the modelled fraction of C allocated to fine roots (wood) at low light levels, while the allocation to foliage remains fairly stable (Fig. 1e). There is a small decrease in the biomass of each of the three pools that occurs at low light levels (Fig. 1f). This limited light sensitivity may arise because, in the numerical experiments of Figs 1e and 1f, the temperature is fixed at a low and thus at a limiting level. There is no sensitivity to the perturbation of specific humidity in either the biomass (Fig. 1h) or the fraction of C allocated to each of the three pools (Fig. 1g).

To quantify the soil moisture stress experienced by vegetation, we use the β soil moisture stress factor as introduced in Eqn. (3). This factor modulates simulated photosynthesis, with a value of unity indicating no soil moisture stress and a value of zero signifying that soil moisture stress is so high it shuts down all physiological responses. Here, biomass in all pools increases with greater soil moisture availability (Fig. 1j). However, the optimisation predicts that the allocation to wood decreases, while the allocation to fine roots increases as soil moisture increases (Fig. 1i). This projection differs from the current understanding that, as soils dry, plants are often observed to increase carbon allocation to roots so they can extract more water (e.g. Broeckx et al., 2014; Hertel et al., 2013; Martin-StPaul et al., 2013). We suggest that these known changes in allometry (i.e. the increase in water-absorbing roots and decrease in transpiring foliage in response to high soil moisture stress) occur to optimise hydraulic conductance and maintain the water transport capacity of plants (e.g. Choat et al., 2012; Magnani et al., 2002; Martin-StPaul et al., 2013). Our model framework, however, optimises productivity based only on available leaf N. Although our optimisation is dependent on soil moisture, via parameter β, it does not explicitly take into account other potential processes, such as maintaining access to soil moisture availability, which may also involve additional elements of optimisation.

Finally, for increasing atmospheric CO_2 concentrations, the new modelling structure forecasts increases in the absolute values of the biomass components (Fig. 1l). However, the fractional allocation of C to fine roots rises with increasing CO_2

https://doi.org/10.5194/egusphere-2026-4392
Preprint. Discussion started: 10 August 2026

reducing the allocation to wood (Fig. 1k), which, encouragingly, aligns with observations (e.g. Iversen et al., 2008; Norby et al., 2004). At higher concentrations of CO_2, from about 300 ppm onwards, the projected extra CO_2 fertilisation for these evergreen pines is minimal. This may be due to the limitations in temperature or nitrogen availability in the soil at this site.

Solving for the cubic polynomial implicit in the optimisation model, while also scanning across potential values of $[N]_f$, and additionally performing perturbation experiments (Fig. 1) is computationally very intensive. Hence, achieving near absolute precision may require further iterations of the numerical solver to avoid the slight "jaggedness" (i.e. loss of smoothness) seen in some panels of Fig. 1.

3.2 Potential overall responses of the revised optimal model to climate change

The motivation behind our analysis is to introduce the effects of environmental drivers to an existing model of optimal carbon allocation that is based on maximising NPP. This enhanced optimal model is designed for equilibrium calculations and is therefore currently unsuitable for high-frequency driver changes, such as those occurring on the seasonal or sub-seasonal timescale. However, it may possess predictive capabilities to describe the important response to imposed climate change on the decadal-to-century timescale, as caused by the human burning of fossil fuels. ESMs are complex modelling frameworks designed to estimate the trajectories of human-induced climate change in different locations and to inform the regular reports of the Intergovernmental Panel on Climate Change (IPCC) (e.g. IPCC, 2021). Although there are many differences among ESM projections, they share two common factors. First, for northern land points, the level of warming per amount of overall mean land warming is substantially higher. Second, the areally-averaged warming over land exceeds that of the global mean warming (the latter calculation also includes the oceans). Both factors are illustrated in the climate "pattern-scaling" analysis of Zelazowski et al. (2018), with their Fig. 2 showing the enhanced northern warming and the parameter ν, which represents the land-sea warming contrast (their Table 1) (see also Fig. 3 of (Huntingford and Mercado, 2016) for the ESM-mean northern warming enhancement). We select a typical value of Finnish warming as 1.3 times higher than overall land warming, alongside a value of $\nu = 1.5$. Given that oceans cover approximately 70% of the planet, this percentage, combined with the ν value, gives that the ratio of global mean land warming to total global warming is also approximately 1.3. By combining the two factors, this yields a representative Finnish warming of approximately $1.3^2 \approx 1.7$ times larger than the global mean warming.

A key summary parameter of the sensitivity of climate change to rising atmospheric greenhouse gases is Equilibrium Climate Sensitivity (ECS) (K), which is the amount of global warming expected for a climate in equilibrium and in response to a doubling of atmospheric CO_2. The latest IPCC report presents ECS ranges as likely between 2.5K and 4.0K, and very likely between 2.0K and 5.0K (Fig. 1.16 of Chen et al. (2021)). Therefore, to account for the maximum variation, we select the very likely bounds and their midpoint (i.e. 3.5K) for ECS and then multiply these by the factor 1.7. This provides an estimate and a range for the mean warming for Finland that corresponds to a climate in equilibrium with a doubling of atmospheric CO_2.

We can now undertake an additional set of simulations to estimate how optimal allocation may adjust under climate change for the Finnish location. We retain the background values for most variables (vertical lines, Fig. 1), except that we use new forcings of temperature rises of 2.0×1.7, 3.5×1.7 or 5.0×1.7. Simultaneously, we prescribe the CO_2 concentration as 794 ppm, which is double that of our control simulations that represent the recent past. Hence, our depiction of climate change is

https://doi.org/10.5194/egusphere-2026-4392
Preprint. Discussion started: 10 August 2026

for an equilibrium state with temperature increases related to a doubling in atmospheric CO_2 concentration. For this illustrative numerical factorial calculation, we assume that there is no change in downward shortwave radiation, humidity and soil moisture stress. In our calculations, we maintain a dependence on different values of available nitrogen, σ_{rM}, but assume that its value is invariant between the current and a future climatic state.

In Fig. 2, we first present the calculated NPP (panel a) for the contemporary period and a future altered climate. Values are shown as a function of σ_{rM}. We base the calculations on an approximation of the current Finnish climate, as well as scenarios for global warming of $2.0, 3.5$ or 5.0 (K) and with a concurrent doubling of atmospheric CO_2. We identify two points of interest. Firstly, the most substantial NPP changes between the present day and a future climate are projected for the higher levels of nitrogen availability (>30 kg N (t fine root)$^{-1}$ yr^{-1}). This numerical finding supports the notion that low nitrogen levels may constrain any CO_2 fertilisation (e.g. Wieder et al., 2015). Second, for higher σ_{rM} values, the projected changes in NPP levels are influenced by ECS. For example, if the planetary ECS is lower, NPP increases, whereas the opposite is true for higher ECS values, suggesting a balance between CO_2 fertilisation and the detrimental effects of elevated temperatures. In panel b of Fig. 2, we show changes in the calculated intermediate variable $[\mathrm{N}]_{\mathrm{f}}$ for the same scenarios.

We present the percentage of C allocated to wood, foliage, and fine roots in panel c of Fig. 2. Values are again shown for the climate forcings of contemporary conditions, and thus the continuous lines in panel c of Fig. 2 are identical to those in panel a of Fig. 1. Under climate change and with higher N availability, the optimisation model predicts a higher fraction of C allocation to wood and foliage but a suppressed fractional allocation to fine roots. We again observed that the estimated values, here of future allocation, are influenced by the ECS value. Next, we consider the effect of climate change on the actual carbon content of foliage and fine roots (Fig. 2; panel d) and wood (Fig. 2; panel e). As for NPP, the changes in carbon stores are not necessarily monotonic for increasing future temperature levels. For the same doubling of atmospheric CO_2, the response curves can fall both above and below the curve for contemporary climate, depending on the ECS values and hence the level of warming. For example, for a doubling of CO_2 and at higher N availability, woody biomass is estimated to increase if global warming corresponds to a lower ECS of just two degrees, but will decrease otherwise (Fig. 2; panel e). Therefore, our model projects a partial suppression of the increase in wood C storage capacity of this mature pine forest if the planet exhibits a strong warming sensitivity to rising atmospheric CO_2.

3.3 Application to BIFoR site

The final numerical calculations with our revised optimal carbon allocation model (Section 2) employ representative values for the BIFoR site (Table 1). We again note that the BIFoR measurement campaign includes a part of the site driven by deliberately elevated atmospheric CO_2 levels, allowing a formal test of the optimisation equations for carbon allocation corresponding to such changed forcing conditions. The average meteorological forcings for the UK location and the parameters needed for the optimal model to be representative of the BIFoR site are presented in Table 1. When forced with the annual mean daytime meteorological conditions of the BIFoR site, ambient CO_2 conditions (397 ppm) and in situ measurements of $V_{cmax,25}$ and $J_{max,25}$ (Table 1), the photosynthesis routine in our revised model projects a top-leaf photosynthetic rate of 14 μmol CO_2 m^{-2} s^{-1}. This calculated value aligns with the measurements for oak trees at the BIFoR site of 12 μmol CO_2 m^{-2} s^{-1}, (C.

https://doi.org/10.5194/egusphere-2026-4392
Preprint. Discussion started: 10 August 2026

Mayoral, unpublished data), also for ambient atmospheric CO_2 concentrations. The calculations forced with raised atmospheric CO_2 are for a value of 550 ppm, which is slightly above the elevated level at the BIFoR site that was actually achieved, while maintaining all other meteorological variables the same as for the computations representing ambient CO_2. Under these conditions, the simulated the photosynthesis rate increases to 15 μmol CO_2 m^{-2} s^{-1}, consistent with the 15 μmol CO_2 m^{-2} s^{-1} values measured for the oaks exposed to higher CO_2 levels at the BIFoR FACE site (C. Mayoral, unpublished data).

The simulation of the variation in NPP, foliar N, carbon allocation fraction and biomass with N availability for the BIFoR site is shown in Fig. 3. For all panels of Fig. 3, the observations are plotted over the range of estimates of N availability (σ_{rM}) for the BIFoR site (see Section 2.2), covering a subset of the "x" axis. The horizontal lines represent the data. Throughout this range of σ_{rM} values, the simulated values of NPP are within a reasonable range of the spread of the data (vertical spread; mean $\pm$ one standard deviation) for both ambient and elevated CO_2. The mean simulated NPP over the range of σ_{rM} values is 6 % higher compared to the mean observations (13.88 t ha^{-1} yr^{-1}, (Norby et al., 2024b)) at ambient CO_2, and 9 % higher compared to mean observations (15.10 t ha^{-1} yr^{-1}, (Norby et al., 2024b)) at elevated CO_2. The calculated leaf N content, $[N]_f$, is closely aligned with the observations (C. Mayoral, unpublished data), with the latter showing values of 2.8 and 2.72 % in ambient and elevated CO_2 respectively (Fig. 3b).

The simulated percentage allocation of carbon to the different pools also shows good absolute agreement with observations for wood and fine roots (52, 36, 13% and 53, 35, 12% to wood, foliage, fine roots, with values for ambient and elevated levels of CO_2 respectively; Norby et al. (2024b)), but the calculations underestimate allocation to foliage (Fig. 3c). Hence, the very small overall projected changes in fractional C allocation for higher atmospheric CO_2 concentrations are seen in both the data and the simulated conditions. It is noted, however, that the signs of these small increments differ between measurements and calculations, with, for instance, the woody fraction projected to decrease while the data suggest a small increase. In simulations (Fig. 3), the difference between responses to ambient versus elevated CO_2 concentrations are suppressed for very high nitrogen availability, σ_{rM}.

Considering the values of actual changes in the biomass pools (Fig. 3d, e), there is again a broad agreement between the model and the data. Specifically, the optimisation model predicts foliage biomass (Fig. 3d) that is in line with the observations (4.08 (s.d 0.41) and 4.47 (s.d 0.46) t ha^{-1} in ambient and elevated CO_2, respectively, calculated as described in Norby et al. (2024b). Critically, both data and model suggest a small increase in foliage biomass for raised atmospheric CO_2. For fine roots (Fig. 3d), the predicted fine root biomass shows substantial variation over the full range of plotted values of σ_{rm}. However, for the overlap region of σ_{rm} values valid at the BIFoR site, there is strong agreement in both magnitude and sign of change for higher atmospheric CO_2 (observed mean fine root biomass 2.05 (s.d 0.24) and 2.87 (s.d 0.50) t ha^{-1} in ambient and elevated CO_2 respectively, calculated as described in Norby et al. (2024b)). The observed wood biomass pool for the oaks at BIFoR is 671.37 (s.d 113.15) t ha^{-1} (Norby et al., 2024a). We consider this ambient value to be also applicable for elevated atmospheric CO_2 at the BIFoR site, since for this large carbon store, it will take a period much longer than the current operation of the BIFoR experiment to reveal the response to higher carbon dioxide levels. The optimisation model approaches this high data value, but with some discrepancy (Fig. 3e). Across the range of σ_{rM} values, the mean simulated wood biomass is 38 % lower under ambient CO_2, and 31 % lower under elevated CO_2 compared to the observed value. The similar modelled NPP (Fig. 3a)

https://doi.org/10.5194/egusphere-2026-4392
Preprint. Discussion started: 10 August 2026

versus the underestimation of woody biomass (Fig. 3e) suggests that the prescribed turnover parameters (e.g. T_S) may benefit from additional measurements. However, some of the model versus data difference in Fig. 3e may also be due to the model simulating sapwood only, where the observations are of total biomass.

4 Discussion and Conclusions

Substantial uncertainty remains regarding the size of terrestrial carbon stores (e.g. Seiler et al., 2022), and how these might change in response to imposed climate change. Currently, there is confidence that land carbon stores are growing and offset a substantial fraction of CO_2 emissions from the human burning of fossil fuels (e.g. Chandra et al., 2022; Sitch et al., 2024; Friedlingstein et al., 2025). However, there is substantial uncertainty about the value of this fraction. Any major reduction in the future level of land carbon storage uptake will imply that a much greater proportion of CO_2 emissions will remain in the atmosphere, thereby increasing global warming. An alternative interpretation is that a reduced capacity for land to absorb emissions implies that lower future "allowable" remaining emissions are compatible with stabilising climate change at a target, such as keeping warming restricted to two degrees above preindustrial levels. Both of these possibilities carry strong policy implications. The primary technique for predicting changes in future land carbon store size involves the use of DGVMs. Such models are numerical frameworks designed to estimate changes at large spatial scales in response to altered near-surface meteorological conditions as atmospheric greenhouse gas concentrations rise. DGVMs contain equations that determine the allocation of carbon available to different components of the overall land store. Instantaneous estimates of available carbon come from the model components that calculate the fluxes of photosynthesis gains and respiration losses, responding to near-surface meteorological and atmospheric conditions.

Much effort by researchers has been directed towards generating datasets of photosynthesis and respiration, which are subsequently available to constrain the parameters of the drivers of DGVMs. These datasets are derived from local, point-scale understanding, such as photosynthesis, and involve experiments conducted over many decades. In more recent decades, there has been a proliferation of FLUXNET eddy covariance measurements (Baldocchi et al., 2001) that record land-atmosphere fluxes, including CO_2 exchanges. These measurements typically have a footprint of many tens of metres. Even more recently, several Earth Observation databases have become available, such as the Normalised Difference Vegetation Index (NDVI), which can serve as a proxy for photosynthetic activity. Another approach is to provide an overall constraint on the global land-atmosphere flux of CO_2, to test the global spatial aggregation of terrestrial models. To achieve this, a residual is calculated, defined as the difference in atmospheric CO_2 once emissions and oceanic drawdown are accounted for (e.g. Le Quere et al., 2013). This difference is attributed to global atmosphere-land CO_2 exchanges.

Yet, despite these many advances in the availability of data to constrain terrestrial simulations, uncertainty remains regarding the precise equation sets and parameters to encode in land models. This uncertainty includes a lack of knowledge about internal allocation processes, as needed in DGVMs. When land models are believed to lack adequate process representation, one possibility is to revisit all data to seek signals and potentially apply very new Artificial Intelligence (AI) methods to reveal the form of any omitted equations (e.g. Huntingford et al., 2025). An alternative possibility, should an equation set be

https://doi.org/10.5194/egusphere-2026-4392
Preprint. Discussion started: 10 August 2026

incomplete, is to consider whether a system might be subject to additional constraints. For terrestrial ecosystems, the extra proposed constraints are often framed as a form of system optimisation, which may produce additional formulas that "close the set of equations". Makela et al. (2008) propose an optimisation model in which the simulated allocation of carbon to wood, foliage, and fine roots is designed to maximise NPP. This maximisation is achieved by varying the intermediate variable of foliage nitrogen, $[N]_f$. In this paper, we extend their model framework to encompass the effects of near-surface meteorological conditions on photosynthesis and respiration, while striving to preserve as much of the original structure as feasible. Our aim is to establish a framework that may be more amenable to eventual inclusion in a full LSM (and, in turn, in an ESM), and critically, that will facilitate an assessment of the implications of optimality assumptions under climate change. Our analysis integrates the impact of climatological conditions into the model of Makela et al. (2008) through the incorporation of well-established photosynthesis and plant respiration components, enabling the study of the effects of their variation under different near-surface conditions. A key advantage of incorporating simulated responses to a broad range of drivers into an optimal model is that it makes the calculations more universal, enabling projections across all regions. This capability includes many locations that lack data for model calibration, for which the optimisation acts as a form of substitute understanding. Geographical applicability for all locations is a key requirement for large-scale numerical LSMs (and ESMs).

We have performed a set of numerical factorial experiments (Fig. 1), perturbing the mean annual environmental conditions from values that may be representative of a Finnish pine and spruce site, thus resembling the calculations of Makela et al. (2008). We first observe that fractional allocations among wood, foliage, and fine roots change considerably with increases in temperature and changes in soil moisture stress. There is much less dependence on individual variations in humidity and downward shortwave radiation. We find that the strongest dependence on atmospheric CO_2 levels occurs when they are reduced to much lower levels than those applicable to contemporary or even preindustrial times (and so our analysis may be of interest to those simulating different periods of paleoclimates). In all cases, except for the top row of Fig. 1, total nitrogen availability, σ_{rM}, is fixed. To simulate human-induced climate change, we also performed a set of factorial experiments in which both temperature and CO_2 are simulated to increase simultaneously (Fig. 2). The largest changes are all associated with higher values of overall nitrogen availability, σ_{rM}, indicating that allocations have more flexibility to adjust when such availability is not limiting (which, based on the understanding from the single factorial simulations in panels c,d and panels k,l of Fig. 1, is particularly controlled by major rises in temperature). For a doubling of atmospheric CO_2, we designate low, medium, and high levels of global warming, roughly based on the range of climate sensitivities of ESMs. Of particular interest is that, for a given fixed value of σ_{rM}, the changes are not necessarily monotonic in relation to climate sensitivity, suggesting balances between CO_2 fertilisation effects and temperature changes, which may be detrimental or beneficial (e.g. in Fig. 2e, for high σ_{rM} values, changes in wood biomass are not linear in response to ECS). A general assessment could be that optimisation may suppress the effects of climate change on allocation, as most changes are minor, leaving the primary determinant of the fractional allocations of NPP as the value of σ_{rM}.

The final set of numerical calculations concerns the application of this framework to a temperate forest at the UK BIFoR location, where a FACE experiment is operational, specifically in the part of the research site that has continuous and intentionally elevated atmospheric CO_2 levels. Therefore, BIFoR data provide an especially valuable test of the revised model

https://doi.org/10.5194/egusphere-2026-4392
Preprint. Discussion started: 10 August 2026

formulation under new environmental forcing regimes. We are encouraged to find that the projected changes in foliage and fine root biomass exhibit similarities in both sign and magnitude to measurements for the BIFoR locations with and without elevated CO_2 (panel d of Fig. 3).

Ultimately, we hope this analysis provides a key intermediate step between the availability of a standalone optimal carbon allocation model and its inclusion in a comprehensive and spatially gridded LSM. LSMs were originally designed to operate as the terrestrial component of weather forecast models, determining energy partitioning through some configuration of the Penman-Monteith equation Monteith (1981). More recently, many of these models have been adapted to operate over modelled timeframes spanning decades to centuries, assessing land-atmosphere CO_2 exchanges and their evolution in response to a changing climate. This extension of capabilities is illustrated by comparing the two model description papers for the JULES land surface model, namely Best et al. (2011) and Clark et al. (2011), which address physical and carbon exchanges, respectively. However, changes in carbon stores will feedback onto these fluxes by modulating levels of photosynthesis and respiration, with implications for policy decisions regarding emissions levels compatible with any predefined temperature scenarios. This necessity to simulate storage changes has driven the development of DGVMs (e.g. Sitch et al., 2008), where their capability to make accurate predictions depends on the accurate representation of allocation. The analysis presented here may support the implementation and testing, in DGVMs, of proposed optimisation strategies by terrestrial ecosystems, starting with the strategy here of maximising NPP.

Our analysis comes with caveats. Although we include a soil moisture response (via parameter β), there are no optimisation-based alterations to the allocation of resources that account for soil water availability. For example, during drought periods, vegetation may enhance carbon availability to fine roots, allowing them to grow larger and, therefore, be more capable of accessing water. In addition, nutrient limitations can combine with water limitations to determine the behaviour of ecosystem allocation (Kleczewski et al., 2012). We also assume that many parameters related to allometry are invariant, such as c_H, which the original analysis of Makela et al. (2008) suggests might vary under climate change. Additionally, a feedback may occur, where altered decomposition rates under a warmer climate, may invalidate the assumption of an invariant rate of N uptake by fine roots, σ_{rM}. Incorporating this into the analysis would require linking it to a soil N model and establishing a functional dependence between dynamic N availability and σ_{rM}. The model of Makela et al. (2008) is an equilibrium model, driven by averaged forcings, and this assumption remains here, and thus including only the effects of average near-surface meteorology. The inclusion of our equations in LSMs, for forcing with climate data, implies that the model will need to respond to interannual variability, or variability on even shorter timescales such as seasonal, daily, or even subdaily. This will necessitate the introduction of inertial equation terms to prevent the model from responding as if varying instantaneous forcings are long-term equilibrium drivers. For instance, the dynamic vegetation components of the JULES model, (Clark et al., 2011), are time-evolving and although a further development of the Makela et al. (2008) model solved a similar optimisation problem in a dynamic case (val), it remains to be resolved how this kind of optimisation can be efficiently applied to non-equilibrium DGVMs. A further numerical strategy is that, should meteorological data be generated at a very high frequency, such as hourly or at the shorter internal clock speeds of calculations by ESMs, the photosynthesis and respiration fluxes may be calculated at those timescales, before being averaged to intermediate timescales of many days. In practice, this would

https://doi.org/10.5194/egusphere-2026-4392
Preprint. Discussion started: 10 August 2026

imply calculating the temporal average of the first underbracketed terms on the right-hand side of Eqns (3) and (8), and then reintroducing these values back into the full equations. Due to multiple nonlinearities in the responses of photosynthesis and respiration, such averaging of high-frequency calculations of these components may generate different estimates than simply using the time-mean value of the meteorological drivers. Arguably, therefore, using photosynthesis and respiration values in the underbracketed terms, calculated at high frequencies and then time-averaged, corresponds to better process representation.

Appropriately averaged conditions could be presented to the allometric optimal model, but it may still require the introduction of transient equation terms. Although FACE experiments, such as BIFoR, provide extremely useful information on the expected changes in land ecosystems as CO_2 increases, these adjustments may not represent a new equilibrium state, with larger ecosystem components responding on decadal or longer timescales. Hence, the introduction of transient equation terms to our model will enable a more rigorous comparison with FACE data. Additionally, our single-variable factorial experiments require careful consideration, as, for example, a prescribed very major increase in temperature (Fig. 1) does not generate levels of very high carbon stores that one might expect for lower latitudes that are warmer, such as the tropics or even drier ecosystems in hot locations. This difference is likely due to light limitation when set at levels applicable to Finland. One further development could be to incorporate an optimisation strategy that accounts for phosphorus and especially for ecosystems that are limited by that nutrient. The JULES model, for example, has recently been updated to account for this geochemical cycle (Nakhavali et al., 2022).

The implementation of our model in an LSM would allow an understanding of the effects of different contemporary background climatic states across the globe, as well as local responses to any imposed climate change, on terrestrial carbon allocation. However, a global implementation will present computational challenges. Central to the analysis by Makela et al. (2008) and the extensions presented here is the necessity of solving a cubic equation, which generally has no exact solution and therefore requires numerical iteration to reach a solution. Even for our single-point analysis, this necessitated substantial iterations to eliminate the bulk of the "jaggedness" associated with parameter variation, as the solutions did not fully converge to the final cubic solution for each parameter value. For our analysis to become a component of an LSM applicable to all land points and frequent simulated time intervals, careful consideration will be needed to ensure numerical efficiency. A final parameterisation-related issue is that our plant respiration description includes a fitting parameter, μ_R, which multiplies the overall Eqn (8), and potentially allows for further fine-tuning based on available measurements. The model for photosynthesis, given by Eqn (3), does not include such a parameter, implicitly assuming that the photosynthesis model is more precise. Users of our new description who wish to fit the photosynthesis component to data could introduce a similar fitting parameter μ_P in front of Eqn (3).

The assumption that terrestrial ecosystems adopt strategies to optimise certain behaviours is a highly appealing concept, as it can be formalised to generate equations that may currently be absent in LSMs. If such strategies are expected to be valid everywhere and remain applicable under changing forcings, this would render LSMs robust both geographically and in projecting the impacts of climate change at each location. We have extended the original optimisation model of Makela et al. (2008), where internal nitrogen concentrations vary to modulate allocations to foliage, fine roots, or wood, in order to maximise NPP. Our extension embeds submodels of photosynthesis, including stomatal opening, and respiration into this structure, which

https://doi.org/10.5194/egusphere-2026-4392
Preprint. Discussion started: 10 August 2026

introduces new dependencies into the optimisation concept of surface temperature, downward shortwave radiation, humidity, soil moisture, and CO_2 concentration. Although we note many caveats in this Section, we believe our approach provides a substantial extension of optimal theory applied to terrestrial carbon allocation. We hope that the closed equation set we present serves as an incentive to test the optimisation assumption within a fully gridded LSM to explore the global implications of land carbon allocation, including under an evolving climate.

5 Code availability

The computer scripts, written with standard python and R modules, that lead to the manuscript diagrams, are available at https://doi.org/10.5281/zenodo.20815389.

Author contributions. C.H. devised the combined model framework, the format of the paper and undertook the calculations. RJO supplied the 'Farquhar' model and provided advice throughout the coupling of it to the optimal model. All authors contributed to the writing of the manuscript.

Competing interests. The authors confirm they have no competing interests.

Acknowledgements. C.H. acknowledges the Natural Environment Research Council (NERC) National Capability award to the U.K. Centre for Ecology and Hydrology (UK-SCAPE, NE/R016429/1). All authors acknowledge the NERC-funded QUINTUS project (NE/S015744/2). R.J.O and L.M.M acknowledge the NERC-funded TerraFirma project (NE/W004895/1). This work was also supported by NERC as part of the NC for Global Challenges programme (NE/X006247/1) delivering National Capability.

https://doi.org/10.5194/egusphere-2026-4392
Preprint. Discussion started: 10 August 2026

References

Baldocchi, D., Falge, E., Gu, L., Olson, R., Hollinger, D., Running, S., Anthoni, P., Bernhofer, C., Davis, K., Evans, R., Fuentes, J., Goldstein, A., Katul, G., Law, B., Lee, X., Malhi, Y., Meyers, T., Munger, W., Oechel, W., U, K., Pilegaard, K., Schmid, H., Valentini, R., Verma, S., Vesala, T., Wilson, K., and Wofsy, S.: FLUXNET: A new tool to study the temporal and spatial variability of ecosystem-scale carbon dioxide, water vapor, and energy flux densities, Bull. Am. Meteorol. Soc., 82, 2415–2434, doi:10.1175/1520-0477(2001)082<2415:FANTTS>2.3.CO;2, 2001.

Best, M. J., Pryor, M., Clark, D. B., Rooney, G. G., Essery, R. L. H., Menard, C. B., Edwards, J. M., Hendry, M. A., Porson, A., Gedney, N., Mercado, L. M., Sitch, S., Blyth, E., Boucher, O., Cox, P. M., Grimmond, C. S. B., and Harding, R. J.: The Joint UK Land Environment Simulator (JULES), model description - Part 1: Energy and water fluxes, Geosci. Model Dev., 4, 677–699, doi:10.5194/gmd-4-677-2011, 2011.

Broeckx, L. S., Verlinden, M. S., Berhongaray, G., Zona, D., Fichot, R., and Ceulemans, R.: The effect of a dry spring on seasonal carbon allocation and vegetation dynamics in a poplar bioenergy plantation, Global Change Biol. Bioenergy, 6, 473–487, doi:10.1111/gcbb.12087, 2014.

Canadell, J. G., Le Quéré, C., Raupach, M. R., Field, C. B., Buitenhuis, E. T., Ciais, P., Conway, T. J., Gillett, N. P., Houghton, R. A., and Marland, G.: Contributions to accelerating atmospheric CO₂ growth from economic activity, carbon intensity, and efficiency of natural sinks, Proc. Natl. Acad. Sci. U.S.A., 104, 18 866–18 870, doi:10.1073/pnas.0702737104, 2007.

Chandra, N., Patra, P. K., Niwa, Y., Ito, A., Iida, Y., Goto, D., Morimoto, S., Kondo, M., Takigawa, M., Hajima, T., and Watanabe, M.: Estimated regional CO2 flux and uncertainty based on an ensemale of atmospheric CO2 inversions, Atmos. Chem. and Phys., 22, 9215–9243, doi:10.5194/acp-22-9215-2022, 2022.

Chen, D., Rojas, M., Samset, B., Cobb, K., Diongue Niang, A., Edwards, P., Emori, S., Faria, S., Hawkins, E., Hope, P., Huybrechts, P., Meinshausen, M., Mustafa, S., Plattner, G.-K., and Tréguier, A.-M.: Framing, Context, and Methods, p. 147–286, Cambridge University Press, Cambridge, United Kingdom and New York, NY, USA, doi:10.1017/9781009157896.003, 2021.

Choat, B., Jansen, S., Brodribb, T. J., Cochard, H., Delzon, S., Bhaskar, R., Bucci, S. J., Feild, T. S., Gleason, S. M., Hacke, U. G., Jacobsen, A. L., Lens, F., Maherali, H., Martinez-Vilalta, J., Mayr, S., Mencuccini, M., Mitchell, P. J., Nardini, A., Pittermann, J., Pratt, R. B., Sperry, J. S., Westoby, M., Wright, I. J., and Zanne, A. E.: Global convergence in the vulnerability of forests to drought, Nature, 491, 752+, doi:10.1038/nature11688, 2012.

Clark, D. B., Mercado, L. M., Sitch, S., Jones, C. D., Gedney, N., Best, M. J., Pryor, M., Rooney, G. G., Essery, R. L. H., Blyth, E., Boucher, O., Harding, R. J., Huntingford, C., and Cox, P. M.: The Joint UK Land Environment Simulator (JULES), model description - Part 2: Carbon fluxes and vegetation dynamics, Geosci. Model Dev., 4, 701–722, doi:10.5194/gmd-4-701-2011, 2011.

Cox, P., Betts, R., Jones, C., Spall, S., and Totterdell, I.: Acceleration of global warming due to carbon-cycle feedbacks in a coupled climate model, Nature, 408, 184–187, doi:10.1038/35041539, 2000.

Ellsworth, D., Reich, P., Naumburg, E., Koch, G., Kubiske, M., and Smith, S.: Photosynthesis, carboxylation and leaf nitrogen responses of 16 species to elevated pCO(2) across four free-air CO2 enrichment experiments in forest, grassland and desert, Global Change Biol., 10, 2121–2138, doi:10.1111/j.1365-2486.2004.00867.x, 2004.

Farquhar, G., Caemmerer, S., and Berry, J.: A biochemicaL-model of photosynthetic CO2 assimilation in leaves of C-3 species, Planta, 149, 78–90, doi:10.1007/BF00386231, 1980.

https://doi.org/10.5194/egusphere-2026-4392
Preprint. Discussion started: 10 August 2026

Field, C. and Mooney, H. A.: The photosynthesis-nitrogen relationship in wild plants, in: On the economy of form and function, edited by Givnish, T., pp. 25–55, Cambridge University Press, Cambridge, United Kingdom and New York, NY, USA, 1986.

Finzi, A. C., Norby, R. J., Calfapietra, C., Gallet-Budynek, A., Gielen, B., Holmes, W. E., Hoosbeek, M. R., Iversen, C. M., Jackson, R. B., Kubiske, M. E., Ledford, J., Liberloo, M., Oren, R., Polle, A., Pritchard, S., Zak, D. R., Schlesinger, W. H., and Ceulemans, R.: Increases in nitrogen uptake rather than nitrogen-use efficiency support higher rates of temperate forest productivity under elevated CO₂, Proc. Natl. Acad. Sci. U.S.A., 104, 14 014–14 019, doi:10.1073/pnas.0706518104, 2007.

Foyer, C. H., Gardner, A., Hayward, S. A. L., Sanchez-Lucas, R., Luna, E., McDonald, J. E., Rumeau, M., Hart, K., Norby, R. J., Mayoral, C., Gauci, V., Smith, A., Hartley, I. P., Crowley, L. M., Sadler, J. P., Ullah, S., and MacKenzie, A. R.: Responses of an Old Deciduous Forest Ecosystem to Elevated CO2, Global Change Biol., 31, e70 355, doi:https://doi.org/10.1111/gcb.70355, 2025.

Franklin, O. and Ågren, G.: Leaf senescence and resorption as mechanisms of maximizing photosynthetic production during canopy development at N limitation, Funct. Ecol., 16, 727–733, doi:10.1046/j.1365-2435.2002.00674.x, 2002.

Franklin, O., Harrison, S. P., Dewar, R., Farrior, C. E., Braennstroem, A., Dieckmann, U., Pietsch, S., Falster, D., Cramer, W., Loreau, M., Wang, H., Makela, A., Rebel, K. T., Meron, E., Schymanski, S. J., Rovenskaya, E., Stocker, B. D., Zaehle, S., Manzoni, S., van Oijen, M., Wright, I. J., Ciais, P., van Bodegom, P. M., Penuelas, J., Hofhansl, F., Terrer, C., Soudzilovskaia, N. A., Midgley, G., and Prentice, I. C.: Organizing principles for vegetation dynamics, Nat. Plants, 6, 444–453, doi:10.1038/s41477-020-0655-x, 2020.

Friedlingstein, P., O'Sullivan, M., Jones, M. W., Andrew, R. M., Hauck, J., Landschutzer, P., Le Quere, C., Li, H., Luijkx, I. T., Olsen, A., Peters, G. P., Peters, W., Pongratz, J., Schwingshackl, C., Sitch, S., Canadell, J. G., Ciais, P., Jackson, R. B., Alin, S. R., Arneth, A., Arora, V., Bates, N. R., Becker, M., Bellouin, N., Berghoff, C. F., Bittig, H. C., Bopp, L., Cadule, P., Campbell, K., Chamberlain, M. A., Chandra, N., Chevallier, F., Chini, L. P., Colligan, T., Decayeux, J., Djeutchouang, L. M., Dou, X., Rojas, C. D., Enyo, K., Evans, W., Fay, A. R., Feely, R. A., Ford, D. J., Foster, A., Gasser, T., Gehlen, M., Gkritzalis, T., Grassi, G., Gregor, L., Gruber, N., Gurses, O., Harris, I., Hefner, M., Heinke, J., Hurtt, G. C., Iida, Y., Ilyina, T., Jacobson, A. R., Jain, A. K., Jarnikova, T., Jersild, A., Jiang, F., Jin, Z., Kato, E., Keeling, R. F., Goldewijk, K. K., Knauer, J., Korsbakken, J. I., Lan, X., Lauvset, S. K., Lefevre, N., Liu, Z., Liu, J., Ma, L., Maksyutov, S., Marland, G., Mayot, N., McGuire, P. C., Metzl, N., Monacci, N. M., Morgan, E. J., Nakaoka, S.-I., Neill, C., Niwa, Y., Nuetzel, T., Olivier, L., Ono, T., Palmer, P. I., Pierrot, D., Qin, Z., Resplandy, L., Roobaert, A., Rosan, T. M., Roedenbeck, C., Schwinger, J., Smallman, T. L., Smith, S. M., Sospedra-Alfonso, R., Steinhoff, T., Sun, Q., Sutton, A. J., Seferian, R., Takao, S., Tatebe, H., Tian, H., Tilbrook, B., Torres, O., Tourigny, E., Tsujino, H., Tubiello, F., van der Werf, G., Wanninkhof, R., Wang, X., Yang, D., Yang, X., Yu, Z., Yuan, W., Yue, X., Zaehle, S., Zeng, N., and Zeng, J.: Global Carbon Budget 2024, Earth Syst. Sci. Data, 17, 965–1039, doi:10.5194/essd-17-965-2025, 2025.

Friedlingstein, P., O'Sullivan, M., Jones, M. W., Andrew, R. M., Bakker, D. C. E., Hauck, J., Landschutzer, P., Le Quere, C., Li, H., Luijkx, I. T., Peters, G. P., Peters, W., Pongratz, J., Schwingshackl, C., Sitch, S., Canadell, J. G., Ciais, P., Aas, K., Alin, S. R., Anthoni, P., Barbero, L., Bates, N. R., Bellouin, N., Benoit-Cattin, A., Berghoff, C. F., Bernardello, R., Bopp, L., Brasika, I. B. M., Chamberlain, M. A., Chandra, N., Chevallier, F., Chini, L. P., Collier, N. O., Colligan, T. H., Cronin, M., Djeutchouang, L. M., Dou, X., Enright, M. P., Enyo, K., Erb, M., Evans, W., Feely, R. A., Feng, L., Ford, D. J., Foster, A., Fransner, F., Gasser, T., Gehlen, M., Gkritzalis, T., Goncalves De Souza, J., Grassi, G., Gregor, L., Gruber, N., Guenet, B., Gurses, O., Harrington, K., Harris, I., Heinke, J., Hurtt, G. C., Iida, Y., Ilyina, T., Ito, A., Jacobson, A. R., Jain, A. K., Jarnikova, T., Jersild, A., Jiang, F., Jones, S. D., Kato, E., Keeling, R. F., Klein Goldewijk, K., Knauer, J., Kong, Y., Korsbakken, J. I., Koven, C., Kunimitsu, T., Lan, X., Liu, J., Liu, Z., Liu, Z., Lo Monaco, C., Ma, L., Marland, G., McGuire, P. C., McKinley, G. A., Melton, J. R., Monacci, N., Monier, E., Morgan, E. J., Munro, D. R., Muller, J. D., Nakaoka, S.-I., Nayagam, L. R., Niwa, Y., Nutzel, T., Olsen, A., Omar, A. M., Pan, N., Pandey, S., Pierrot, D., Qin, Z., Regnier, P., Rehder, G., Resplandy, L., Roobaert, A., Rosan, T. M., Rodenbeck, C., Schwinger, J., Skjelvan, I., Smallman, T. L., Spada, V., Sreeush, M. G., Sun, Q., Sutton,

https://doi.org/10.5194/egusphere-2026-4392
Preprint. Discussion started: 10 August 2026

A. J., Sweeney, C., Swingedouw, D., Seferian, R., Takao, S., Tatebe, H., Tian, H., Tian, X., Tilbrook, B., Tsujino, H., Tubiello, F., van Ooijen, E., van der Werf, G. R., van de Velde, S. J., Walker, A. P., Wanninkhof, R., Yang, X., Yuan, W., Yue, X., and Zeng, J.: Global Carbon Budget 2025, Earth Syst. Sci. Data, 18, 3211–3288, doi:10.5194/essd-18-3211-2026, 2026.

Gardner, A., Ellsworth, D. S., Crous, K. Y., Pritchard, J., and MacKenzie, A. R.: Is photosynthetic enhancement sustained through three years of elevated CO2 exposure in 175-year-old Quercus robur?, Tree Physiol., 42, 130–144, doi:10.1093/treephys/tpab090, 2022.

Harper, A. B., Cox, P. M., Friedlingstein, P., Wiltshire, A. J., Jones, C. D., Sitch, S., Mercado, L. M., Groenendijk, M., Robertson, E., Kattge, J., Boenisch, G., Atkin, O. K., Bahn, M., Cornelissen, J., Niinemets, U., Onipchenko, V., Penuelas, J., Poorter, L., Reich, P. B., Soudzilovskaia, N. A., and van Bodegom, P.: Improved representation of plant functional types and physiology in the Joint UK Land Environment Simulator (JULES v4.2) using plant trait information, Geosci. Model Dev., 9, 2415–2440, doi:10.5194/gmd-9-2415-2016, 2016.

Harrison, S. P., Cramer, W., Franklin, O., Prentice, I. C., Wang, H., Brannstrom, A., de Boer, H., Dieckmann, U., Joshi, J., Keenan, T. F., Lavergne, A., Manzoni, S., Mengoli, G., Morfopoulos, C., Penuelas, J., Pietsch, S., Rebel, K. T., Ryu, Y., Smith, N. G., Stocker, B. D., and Wright, I. J.: Eco-evolutionary optimality as a means to improve vegetation and land-surface models, New Phytol., 231, 2125–2141, doi:10.1111/nph.17558, 2021.

Hart, K. M., Curioni, G., Blaen, P., Harper, N. J., Miles, P., Lewin, K. F., Nagy, J., Bannister, E. J., Cai, X. M., Thomas, R. M., Krause, S., Tausz, M., and MacKenzie, A. R.: Characteristics of free air carbon dioxide enrichment of a northern temperate mature forest, Global Change Biol., 26, 1023–1037, doi:10.1111/gcb.14786, 2020.

Hertel, D., Strecker, T., Mueller-Haubold, H., and Leuschner, C.: Fine root biomass and dynamics in beech forests across a precipitation gradient - is optimal resource partitioning theory applicable to water-limited mature trees?, J. Ecol., 101, 1183–1200, doi:10.1111/1365-2745.12124, 2013.

Hilbert, D. W.: Optimization of plant-root - shoot ratios and internal nitrogen concentration, Ann. Bot., 66, 91–99, doi:10.1093/oxfordjournals.aob.a088005, 1990.

Huntingford, C. and Mercado, L. M.: High chance that current atmospheric greenhouse concentrations commit to warmings greater than 1.5 degrees C over land, Sci. Rep., 6, 30 294, doi:10.1038/srep30294, 2016.

Huntingford, C., Burke, E. J., Jones, C. D., Jeffers, E. S., and Wiltshire, A. J.: Nitrogen cycle impacts on CO₂ fertilisation and climate forcing of land carbon stores, Environ. Res. Lett., 17, 044 072, doi:10.1088/1748-9326/ac6148, 2022.

Huntingford, C., Nicoll, A. J., Klein, C., and Ahmad, J. A.: Potential for equation discovery with AI in the climate sciences, Earth Syst. Dyn., 16, 475–495, doi:10.5194/esd-16-475-2025, 2025.

IPCC: Climate Change 2013: The Physical Science Basis. Contribution of Working Group I to the Fifth Assessment Report of the Intergovernmental Panel on Climate Change, Cambridge University Press, Cambridge, United Kingdom and New York, NY, USA, doi:10.1017/CBO9781107415324, www.climatechange2013.org, 2013.

IPCC: Climate Change 2021: The Physical Science Basis. Contribution of Working Group I to the Sixth Assessment Report of the Intergovernmental Panel on Climate Change, Cambridge University Press, Cambridge, United Kingdom and New York, NY, USA, doi:10.1017/9781009157896, 2021.

Iversen, C. M., Ledford, J., and Norby, R. J.: CO₂ enrichment increases carbon and nitrogen input from fine roots in a deciduous forest, New Phytol., 179, 837–847, doi:10.1111/j.1469-8137.2008.02516.x, 2008.

https://doi.org/10.5194/egusphere-2026-4392
Preprint. Discussion started: 10 August 2026

Kleczewski, N. M., Herms, D. A., and Bonello, P.: Nutrient and water availability alter belowground patterns of biomass allocation, carbon partitioning, and ectomycorrhizal abundance in Betula nigra, Trees-Struct. and Funct., 26, 525–533, doi:10.1007/s00468-011-0613-3, 2012.

Le Quere, C., Andres, R. J., Boden, T., Conway, T., Houghton, R. A., House, J. I., Marland, G., Peters, G. P., van der Werf, G. R., Ahlstrom, A., Andrew, R. M., Bopp, L., Canadell, J. G., Ciais, P., Doney, S. C., Enright, C., Friedlingstein, P., Huntingford, C., Jain, A. K., Jourdain, C., Kato, E., Keeling, R. F., Goldewijk, K. K., Levis, S., Levy, P., Lomas, M., Poulter, B., Raupach, M. R., Schwinger, J., Sitch, S., Stocker, B. D., Viovy, N., Zaehle, S., and Zeng, N.: The global carbon budget 1959-2011, Earth Syst. Sci. Data, 5, 165–185, doi:10.5194/essd-5-165-2013, 2013.

Litton, C. M., Raich, J. W., and Ryan, M. G.: Carbon allocation in forest ecosystems, Global Change Biol., 13, 2089–2109, doi:10.1111/j.1365-2486.2007.01420.x, 2007.

Luo, X., Keenan, T. F., Chen, J. M., Croft, H., Colin Prentice, I., Smith, N. G., Walker, A. P., Wang, H., Wang, R., Xu, C., and Zhang, Y.: Global variation in the fraction of leaf nitrogen allocated to photosynthesis, Nat. Commun., 12, 4866, doi:10.1038/s41467-021-25163-9, 2021.

MacKenzie, A. R., Krause, S., Hart, K. M., Thomas, R. M., Blaen, P. J., Hamilton, R. L., Curioni, G., Quick, S. E., Kourmouli, A., Hannah, D. M., Comer-Warner, S. A., Brekenfeld, N., Ullah, S., and Press, M. C.: BIFoR FACE: Water-soil-vegetation-atmosphere data from a temperate deciduous forest catchment, including under elevated CO2, Hydrol. Processes, 35, e14 096, doi:10.1002/hyp.14096, 2021.

Magnani, F., Grace, J., and Borghetti, M.: Adjustment of tree structure in response to the environment under hydraulic constraints, Funct. Ecol., 16, 385–393, doi:10.1046/j.1365-2435.2002.00630.x, 2002.

Makela, A., Valentine, H. T., and Helmisaari, H.-S.: Optimal co-allocation of carbon and nitrogen in a forest stand at steady state, New Phytol., 180, 114–123, doi:10.1111/j.1469-8137.2008.02558.x, 2008.

Martin-StPaul, N. K., Limousin, J.-M., Vogt-Schilb, H., Rodriguez-Calcerrada, J., Rambal, S., Longepierre, D., and Misson, L.: The temporal response to drought in a Mediterranean evergreen tree: comparing a regional precipitation gradient and a throughfall exclusion experiment, Global Change Biol., 19, 2413–2426, doi:10.1111/gcb.12215, 2013.

Medlyn, B. E., Duursma, R. A., Eamus, D., Ellsworth, D. S., Prentice, I. C., Barton, C. V. M., Crous, K. Y., de Angelis, P., Freeman, M., and Wingate, L.: Reconciling the optimal and empirical approaches to modelling stomatal conductance, Global Change Biol., 17, 2134–2144, doi:10.1111/j.1365-2486.2010.02375.x, 2011.

Medlyn, B. E., Zaehle, S., De Kauwe, M. G., Walker, A. P., Dietze, M. C., Hanson, P. J., Hickler, T., Jain, A. K., Luo, Y., Parton, W., Prentice, I. C., Thornton, P. E., Wang, S., Wang, Y.-P., Weng, E., Iversen, C. M., McCarthy, H. R., Warren, J. M., Oren, R., and Norby, R. J.: Using ecosystem experiments to improve vegetation models, Nat. Clim. Change, 5, 528–534, doi:10.1038/nclimate2621, 2015.

Monteith, J.: Evaporation and surface-temperature, Q. J. R. Meteorolog. Soc., 107, 1–27, doi:10.1256/smsqj.45101, 1981.

Nakhavali, M. A., Mercado, L. M., Hartley, I. P., Sitch, S., Cunha, F. V., di Ponzio, R., Lugli, L. F., Quesada, C. A., Andersen, K. M., Chadburn, S. E., Wiltshire, A. J., Clark, D. B., Ribeiro, G., Siebert, L., Moraes, A. C. M., Schmeisk Rosa, J., Assis, R., and Camargo, J. L.: Representation of the phosphorus cycle in the Joint UK Land Environment Simulator (vn5.5_JULES-CNP), Geosci. Model Dev., 15, 5241–5269, doi:10.5194/gmd-15-5241-2022, 2022.

Norby, R., Ledford, J., Reilly, C., Miller, N., and O'Neill, E.: Fine-root production dominates response of a deciduous forest to atmospheric CO₂ enrichment, Proc. Natl. Acad. Sci. U.S.A., 101, 9689–9693, doi:10.1073/pnas.0403491101, 2004.

https://doi.org/10.5194/egusphere-2026-4392
Preprint. Discussion started: 10 August 2026

Norby, R. J., Loader, N. J., Mayoral, C., Ullah, S., Curioni, G., Smith, A. R., Reay, M. K., and van Wijngaarden, K.: Data from: Enhanced woody biomass production in a mature temperate forest under elevated CO2, https://datadryad.org/dataset/doi:10.5061/dryad.z612jm6jw, [Dataset] Accessed August 2025, 2024a.

Norby, R. J., Loader, N. J., Mayoral, C., Ullah, S., Curioni, G., Smith, A. R., Reay, M. K., van Wijngaarden, K., Amjad, M. S., Brettle, D., Crockatt, M. E., Denny, G., Grzesik, R. T., Hamilton, R. L., Hart, K. M., Hartley, I. P., Jones, A. G., Kourmouli, A., Larsen, J. R., Shi, Z., Thomas, R. M., and Mackenzie, A. R.: Enhanced woody biomass production in a mature temperate forest under elevated CO2, Nat. Clim. Change, 14, 983–988, doi:10.1038/s41558-024-02090-3, 2024b.

Oliver, R. J., Mercado, L. M., Clark, D. B., Huntingford, C., Taylor, C. M., Vidale, P. L., McGuire, P. C., Todt, M., Folwell, S., Shamsudheen Semeena, V., and Medlyn, B. E.: Improved representation of plant physiology in the JULES-vn5.6 land surface model: photosynthesis, stomatal conductance and thermal acclimation, Geosci. Model Dev., 15, 5567–5592, doi:10.5194/gmd-15-5567-2022, 2022.

Seiler, C., Melton, J. R., Arora, V. K., Sitch, S., Friedlingstein, P., Anthoni, P., Goll, D., Jain, A. K., Joetzjer, E., Lienert, S., Lombardozzi, D., Luyssaert, S., Nabel, J. E. M. S., Tian, H., Vuichard, N., Walker, A. P., Yuan, W., and Zaehle, S.: Are Terrestrial Biosphere Models Fit for Simulating the Global Land Carbon Sink?, J. Adv. Model. Earth Syst., 14, e2021MS002 946, doi:10.1029/2021MS002946, 2022.

Sellers, P., Berry, J., Collatz, G., Field, C., and Hall, F.: Canopy reflectance, photosynthesis, and transpiration .3. A reanalysis using improved leaf models and a new canopy integration scheme, Remote Sens. Environ., 42, 187–216, doi:10.1016/0034-4257(92)90102-P, 1992.

Sitch, S., Huntingford, C., Gedney, N., Levy, P. E., Lomas, M., Piao, S. L., Betts, R., Ciais, P., Cox, P., Friedlingstein, P., Jones, C. D., Prentice, I. C., and Woodward, F. I.: Evaluation of the terrestrial carbon cycle, future plant geography and climate-carbon cycle feedbacks using five Dynamic Global Vegetation Models (DGVMs), Global Change Biol., 14, 2015–2039, doi:10.1111/j.1365-2486.2008.01626.x, 2008.

Sitch, S., O'Sullivan, M., Robertson, E., Friedlingstein, P., Albergel, C., Anthoni, P., Arneth, A., Arora, V. K., Bastos, A., Bastrikov, V., Bellouin, N., Canadell, J. G., Chini, L., Ciais, P., Falk, S., Harris, I., Hurtt, G., Ito, A., Jain, A. K., Jones, M. W., Joos, F., Kato, E., Kennedy, D., Goldewijk, K. K., Kluzek, E., Knauer, J., Lawrence, P. J., Lombardozzi, D., Melton, J. R., Nabel, J. E. M. S., Pan, N., Peylin, P., Pongratz, J., Poulter, B., Rosan, T. M., Sun, Q., Tian, H., Walker, A. P., Weber, U., Yuan, W., Yue, X., and Zaehle, S.: Trends and Drivers of Terrestrial Sources and Sinks of Carbon Dioxide: An Overview of the TRENDY Project, Global Biogeochem. Cycles, 38, e2024GB008 102, doi:10.1029/2024GB008102, 2024.

Wieder, W. R., Cleveland, C. C., Smith, W. K., and Todd-Brown, K.: Future productivity and carbon storage limited by terrestrial nutrient availability, Nat. Geosci., 8, 441–444, doi:10.1038/NGEO2413, 2015.

Zaehle, S.: Terrestrial nitrogen - carbon cycle interactions at the global scale, Philos. Trans. R. Soc. London, Ser. B, 368, 20130 125, doi:10.1098/rstb.2013.0125, 2013.

Zelazowski, P., Huntingford, C., Mercado, L. M., and Schaller, N.: Climate pattern-scaling set for an ensemble of 22 GCMs - adding uncertainty to the IMOGEN version 2.0 impact system, Geosci. Model Dev., 11, 541–560, doi:10.5194/gmd-11-541-2018, 2018.

https://doi.org/10.5194/egusphere-2026-4392
Preprint. Discussion started: 10 August 2026

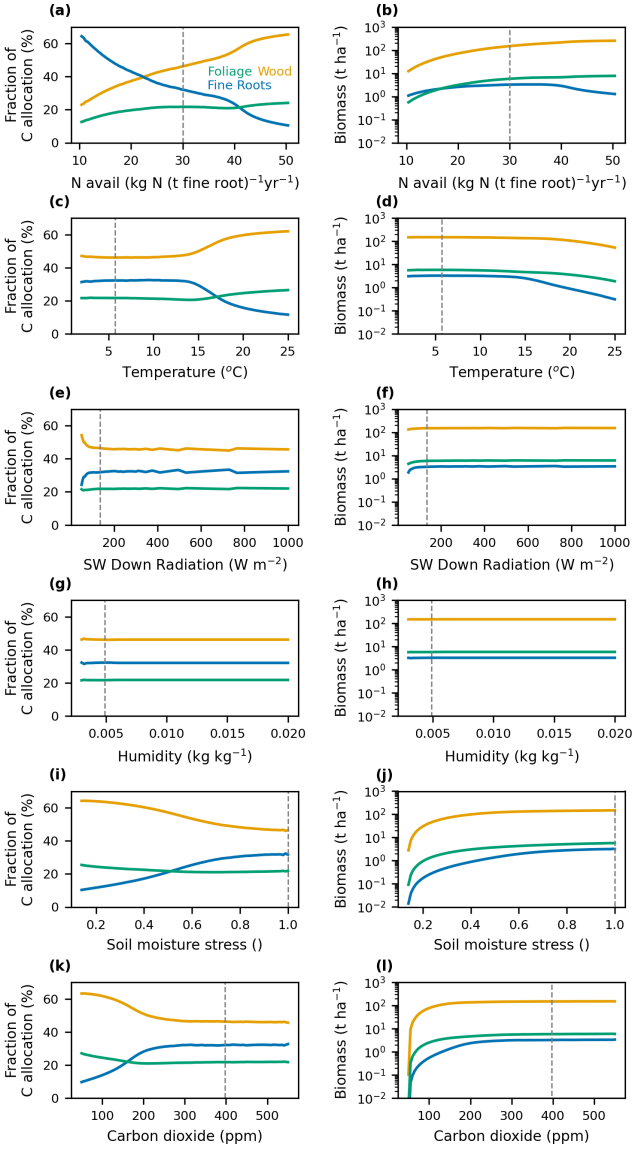

Figure 1. Dependencies of the optimal model, as modified with our added descriptions of photosynthesis and respiration, and under perturbed environmental conditions. The unperturbed conditions are applicable to a Finnish mature evergreen pine forest. The left-hand column shows the fractional allocation of the rate of production, G, into the three components of wood, foliage, and fine roots. Values are of λ_w, λ_f and λ_r are expressed as percentages. The right-hand column displays the dry biomass of each of these three components, W_w, W_f and W_r. In rows from top to bottom, perturbations are applied away from default values in prescribed overall nitrogen availability σ_{rM}, temperature T, downward shortwave radiation I, specific humidity q, soil moisture stress scaling factor β (and where a value of unity is no water stress) and carbon dioxide concentration c_a. The default value for available nitrogen takes the midpoint of the range considered, i.e. 30.0 $\sigma_{rM} = 30$ kg N (t fine root)$^{-1}$ yr^{-1}. The other default values, mirroring the analysis of Makela et al. (2008), for temperature are 5.0 ^{o}C, downward shortwave radiation of 135 W m^{-2}, specific humidity of 0.005 kg kg^{-1}, no soil moisture stress (i.e. $\beta = 1$), and CO_2 concentration of 397 ppm. These default values are marked as vertical grey dashed lines. Please note the logarithmic vertical axis in the second column.

https://doi.org/10.5194/egusphere-2026-4392
Preprint. Discussion started: 10 August 2026

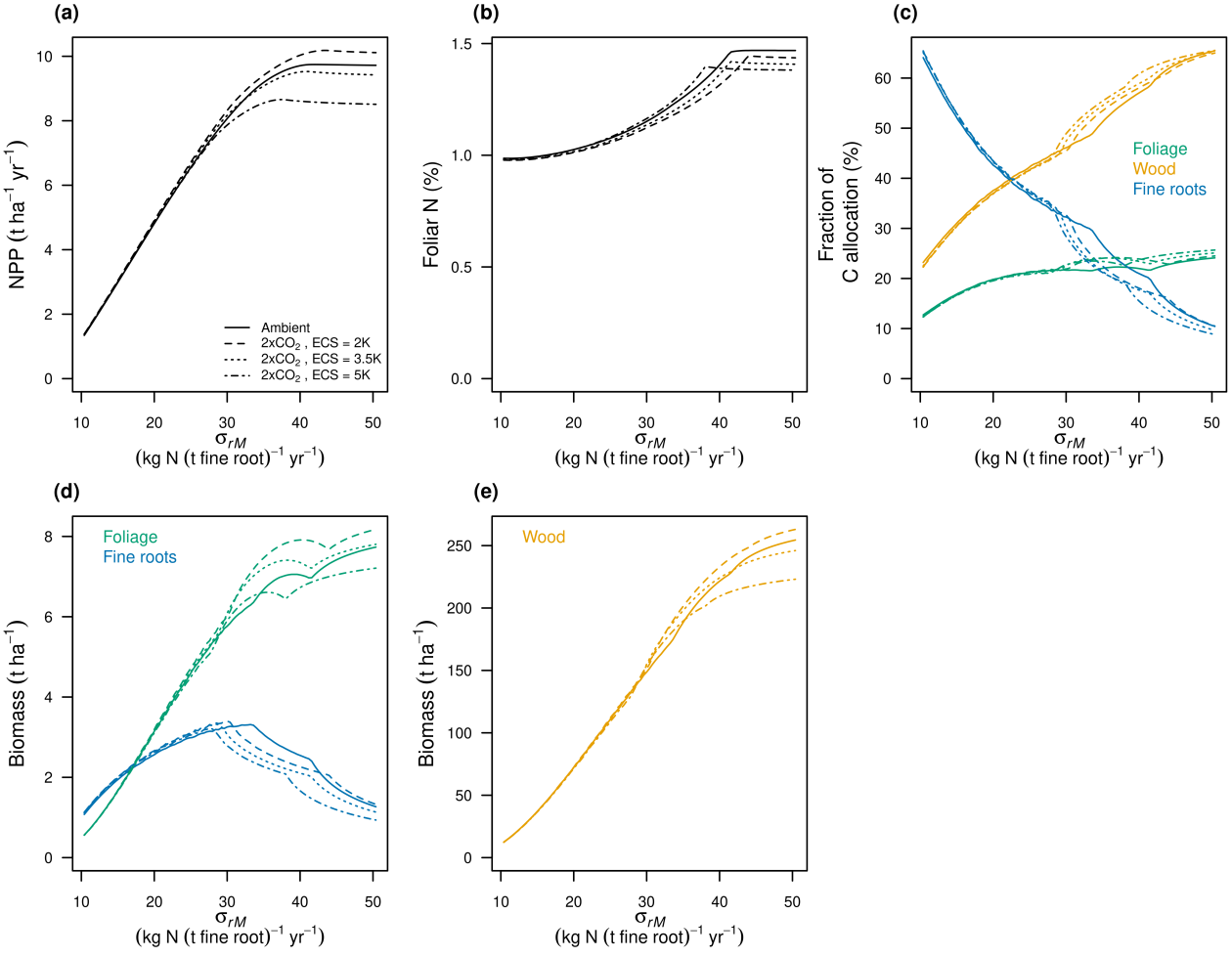

Figure 2. Combined simulated effects of global warming and a rise in atmospheric CO_2 as forcings of the optimal model, using parameters representative of Finnish mature evergreen pine trees. Model behaviour is illustrated for ambient conditions (solid line), 2xCO_2 alongside a 2K rise in global warming (dashed line), 2xCO_2 alongside a 3.5K rise in global warming (dotted line) and 2xCO_2 alongside a 5K rise in global warming (dash-dot line). Actual local temperature increases prescribed to the model are greater, capturing the faster warming over land and in locations at higher latitudes, such as Finland. Panel a is simulated Net Primary Productivity (NPP), reported as dry matter (that is, NPP = $G = Y(P - R_m)$), panel b presents foliar (leaf) nitrogen, $[\mathrm{N}]_\mathrm{f}$, and panel c presents the fractional allocation of carbon to foliage (green), wood (yellow) and fine roots (blue). Panel d shows simulated foliage and fine root biomass, and panel e shows simulated wood biomass, with both panels d and e also reporting in units of dry matter. All calculations are presented as a function of nitrogen availability, σ_{rM}. The ambient curves (with continuous line styles) in panel c are the same as those in Fig. 1a. Similarly, the continous lines in panels d and e are identical to those in Fig. 1b

https://doi.org/10.5194/egusphere-2026-4392
Preprint. Discussion started: 10 August 2026

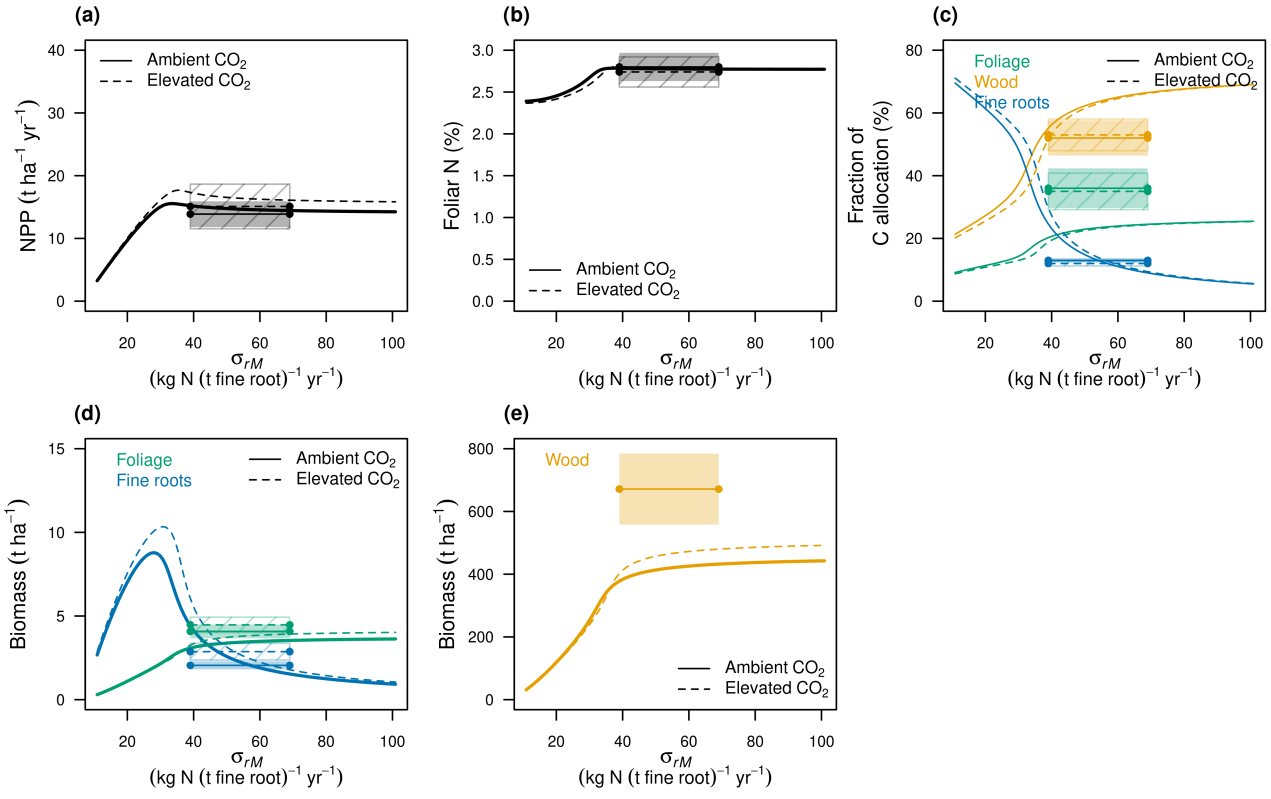

Figure 3. Application of the optimal model using parameters for mature oak trees (*Quercus robur*) valid for the UK BIFoR site, a mature broadleaf deciduous temperate forest, which hosts a FACE experiment. Model projections are shown for ambient CO_2 concentration (397 ppm, solid lines) and elevated atmospheric CO_2 concentration (550 ppm, dashed lines) in all panels, and for different prescribed values of nitrogen availability (σ_{rM}). Mean observed values are shown by the horizontal lines drawn over the range of σ_{rM} data values applicable to the BIFoR site. For the observations, at ambient CO_2, the means are represented by the horizontal solid lines, and $\pm$ 1 s.d. is the solid vertical shading. For elevated CO_2, the observed means are represented by the dashed horizontal lines, and $\pm$ 1 s.d. is the vertical hatched shading. Panel a displays simulated Net Primary Productivity (NPP), reported as dry matter (that is, NPP = $G = Y(P - R_m)$), panel b presents foliar (leaf) nitrogen, $[\mathrm{N}]_\mathrm{f}$, and panel c presents the fractional allocation of carbon to foliage (green), wood (yellow) and fine roots (blue). Panel d shows simulated foliage and fine root biomass, while panel e shows simulated wood biomass, with both panels d and e also reporting in units of dry matter.